

1 The Evolution of Siphonophore Tentilla as Specialized 2 Tools for Prey Capture

3 Alejandro Damian-Serrano^{1,‡}, Steven H.D. Haddock², Casey W. Dunn¹

**4 ¹ Yale University, Department of Ecology and Evolutionary Biology, 165 Prospect St.,
5 New Haven, CT 06520, USA**

**6 ² Monterey Bay Aquarium Research Institute, 7700 Sandholdt Rd., Moss Landing, CA
7 95039, USA**

**8 ‡ Corresponding author: Alejandro Damian-Serrano, email: alejandro.damianserrano@
9 yale.edu**

10 Abstract

**11 Predators have evolved dedicated body parts to capture and subdue prey. As different
12 predators specialize on distinct prey taxa, their tools for prey capture diverge into a variety
13 of adaptive forms. Studying the evolution of predation is facilitated by a predator clade
14 with structures used exclusively for prey capture and with significant morphological varia-
15 tion. Siphonophores, a clade of colonial cnidarians, satisfy these criteria particularly well,
16 capturing prey with their tentilla (tentacle side branches). Earlier work has shown that
17 extant siphonophore diets correlate with the different morphologies and sizes of their tentilla
18 and nematocysts. We hypothesize that evolutionary specialization on different prey types
19 has driven the phenotypic evolution of these characters. To test this hypothesis, we: (1)
20 measured multiple morphological traits from fixed siphonophore specimens using microscopy
21 and high-speed video techniques, (2) built a phylogenetic tree of 45 species, and (3) analyzed
22 the evolutionary associations between siphonophore nematocyst characters and prey type
23 data from the literature. Our results show that siphonophore tentillum structure has strong
24 evolutionary associations with prey type and size specialization, and suggest that shifts
25 between prey-type specializations are linked to shifts in tentillum and nematocyst size and**

26 shape. In addition, we generated hypotheses about the diets of understudied siphonophore
27 species based on these characters. Thus, the evolutionary history of tentilla shows that
28 siphonophores are an example of ecological niche diversification via morphological innovation
29 and evolution. This study contributes to understanding how morphological evolution has
30 shaped present-day oceanic food webs.

31 **Keywords**

32 Siphonophores, tentilla, nematocysts, predation, specialization, character evolution

33

34 Most animal predators have characteristic biological tools that they use to capture and
35 subdue prey. Raptors have claws and beaks, snakes have fangs, wasps have stingers, and
36 cnidarians have nematocyst-laden tentacles. The functional morphology of these structures
37 tend to be finely attuned to their ability to successfully capture specific prey (Schmitz
38 2017). Long-term adaptive evolution in response to the defense mechanisms of the prey (*e.g.*
39 avoidance, escape, protective barriers) leads to modifications that can counter those defenses
40 The more specialized the diet of a predator is, the more specialized its tools need to be to
41 meet the specific challenges posed by the prey. Understanding the relationships between
42 predatory specializations and morphological specializations is necessary to contextualize the
43 phenotypic diversity of predators, and to quantify the importance of ecological diversification
44 in generating this diversity.

45 Siphonophores (Cnidaria : Hydrozoa) are a clade of organisms bearing modular structures
46 that are exclusively used for prey capture: the tentilla (Fig. 1). These present a significant
47 morphological variation across species (Mapstone 2014) (Fig. 2), which makes them an
48 ideal system to study the relationships between functional traits and prey specialization. A
49 siphonophore is a colony bearing many feeding polyps (Fig. 1), each with a single tentacle,
50 which branches into several tentilla carrying the functional cnidocytes (specialized neural cells

51 carrying nematocysts, the stinging capsules). Unlike most other cnidarians, siphonophores
52 carry their tentacle nematocysts in extremely complex and organized batteries (Skaer 1988)
53 built into their tentilla. While nematocyst batteries and clusters in other cnidarians are simple
54 static scaffolds for cnidocytes, siphonophore tentilla have their own reaction mechanism,
55 triggered upon encounter with prey. When it fires, a tentillum undergoes an extremely fast
56 conformational change that wraps it around the prey, maximizing the surface area of contact
57 for nematocysts to fire on the prey (Mackie et al. 1987). In addition, some species have
58 elaborate fluorescent and bioluminescent lures on their tentilla to attract prey with aggressive
59 mimicry (Purcell 1980; Haddock et al. 2005; Haddock and Dunn 2015).

60 Many siphonophore species inhabit the deep pelagic ocean, which spans from ~200m to
61 the oceanic seafloor. This habitat has fairly homogeneous physical conditions and stable
62 zooplankton abundances and composition (Robison 2004). With a relatively predictable
63 prey availability, ecological theory would predict evolution to drive coexisting siphonophore
64 lineages towards specialization, increasing their feeding efficiencies and reducing interspecific
65 competition (Simpson 1944; Hardin 1960; Hutchinson 1961). If this prediction holds true,
66 we expect the prey capture apparatus morphologies of siphonophores to diversify with the
67 evolution of increased specialization on a variety of prey types in different siphonophore
68 lineages.

69 Specialization is often thought to be an evolutionary ‘dead end’, meaning that specialized
70 lineages are unlikely to evolve into generalists or to shift the resource for which they are
71 specialized (Futuyma and Moreno 1988). However, recent studies have found that interspecific
72 competition can favor the evolution of resource generalism (Stireman-III 2005; Johnson et
73 al. 2009) and resource switching (Hoberg and Brooks 2008). Here we examine three
74 alternative hypotheses on siphonophore trophic specialization: (1) predatory specialists
75 evolved from generalist ancestors; (2) predatory specialists evolved from ancestral predators
76 which specialized on a different resource, switching their primary prey type; and (3) predatory
77 generalists evolved from specialist ancestors.

78 The study of siphonophore tentilla and diets has been limited in the past due to the
79 inaccessibility of their oceanic habitat and the difficulties associated with the collection of
80 fragile siphonophores. Thus, the morphological diversity of tentilla has only been characterized
81 for a few taxa, and their evolutionary history remains largely unexplored. Contemporary
82 underwater sampling technology provides an unprecedented opportunity to explore the trophic
83 ecology (Choy et al. 2017) and functional morphology (Costello et al. 2015) of siphonophores.
84 In addition, well-supported phylogenies based on molecular data are now available for these
85 organisms (Munro et al. 2018). These advances allow for the examination of relationships
86 between modern siphonophore form, function, and ecology, as well as reconstructing their
87 evolutionary history.

88 The few pioneering studies that have addressed the relationships between tentilla and
89 diet suggest that siphonophores are a robust system for the study of predatory specialization
90 via morphological diversification. (Purcell 1984) and (Purcell and Mills 1988) showed clear
91 relationships between diet, tentillum, and nematocyst characters in co-occurring epipelagic
92 siphonophores. These correlations, while studied for a small subset of extant epipelagic
93 siphonophore species, might be generalizable to all siphonophores. We hypothesize that
94 these relationships reflect correlated evolution between prey selection and tentillum (and
95 nematocyst) traits. Furthermore, we hypothesize that with an extensive characterization of
96 tentilla morphology, we can generate hypotheses about the diets of understudied siphonophore
97 species.

98 In addition, our study design allows us to address other interesting questions about the
99 morphology and evolution of these unique structures. In particular, we aim to address the
100 evolutionary origins of giant tentilla, the character integration of tentilla, the evolution of
101 the extreme shapes of siphonophore nematocysts (Thomason 1988), and the mechanical
102 implications of tentillum morphologies on cnidoband discharge.

103 In this study, we characterize the morphological diversity of tentilla and their nematocysts
104 across a broad variety of shallow and deep sea siphonophore species using modern imaging

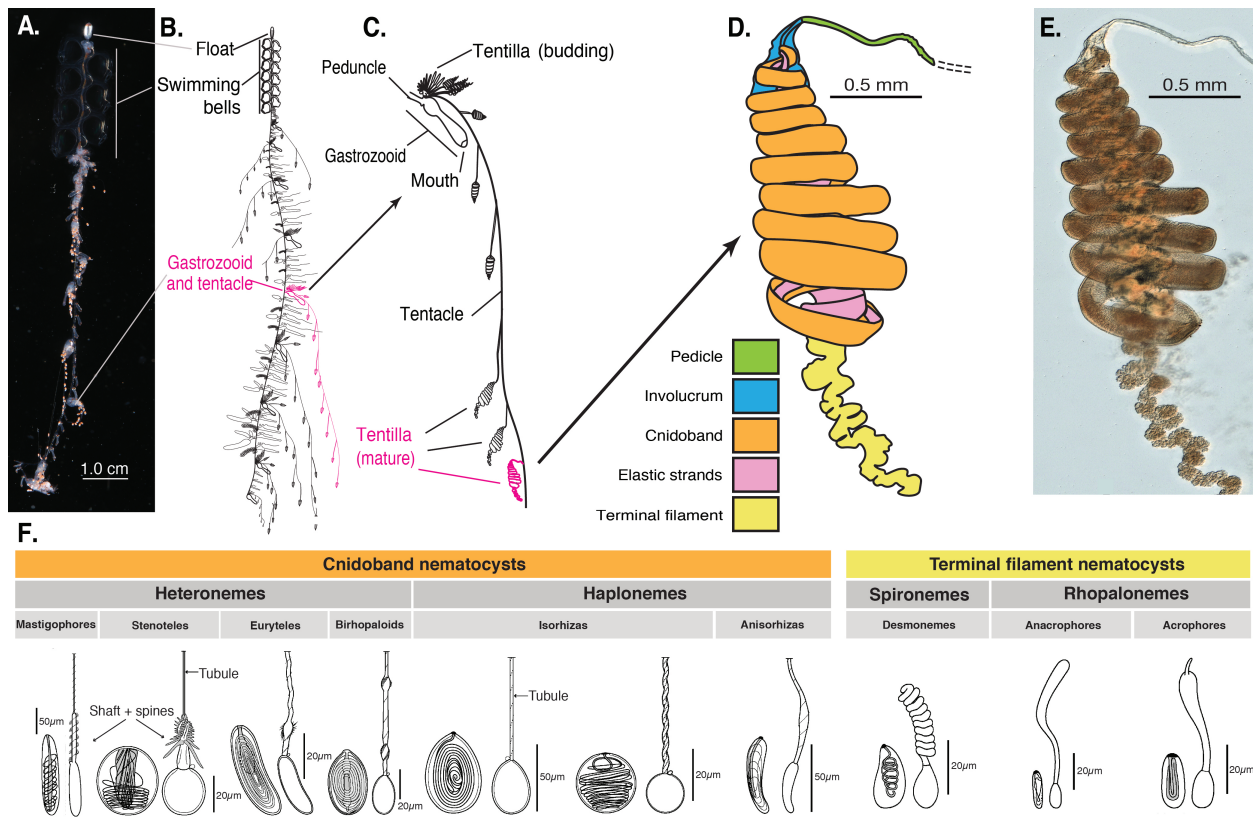


Figure 1: Siphonophore anatomy. A - *Nanomia* sp. siphonophore colony (photo by Catriona Munro). B,C - Illustration of a *Nanomia* colony, gastrozooid, and tentacle (by Freya Goetz). D - *Nanomia* sp. Tentillum illustration and main parts. E - Differential interference contrast micrograph of the tentillum illustrated in D. F - Nematocyst types (illustration reproduced with permission from Mapstone 2014), hypothesized homologies, and locations in the tentillum. Undischarged to the left, discharged to the right.

105 technologies, we expand the phylogenetic tree of siphonophores by combining a broad taxon
 106 sampling of ribosomal gene sequences with a transcriptome-based backbone tree, and we
 107 explore the evolutionary histories and correlations among diet, tentillum, and nematocyst
 108 characters.

109 Methods

110 *Tentillum morphology* – The morphological work was carried out on siphonophore specimens
 111 fixed in 4% formalin from the Yale Peabody Museum Invertebrate Zoology (YPM-IZ) collection
 112 (accession numbers in Appendix 1). These specimens were collected intact across many years of

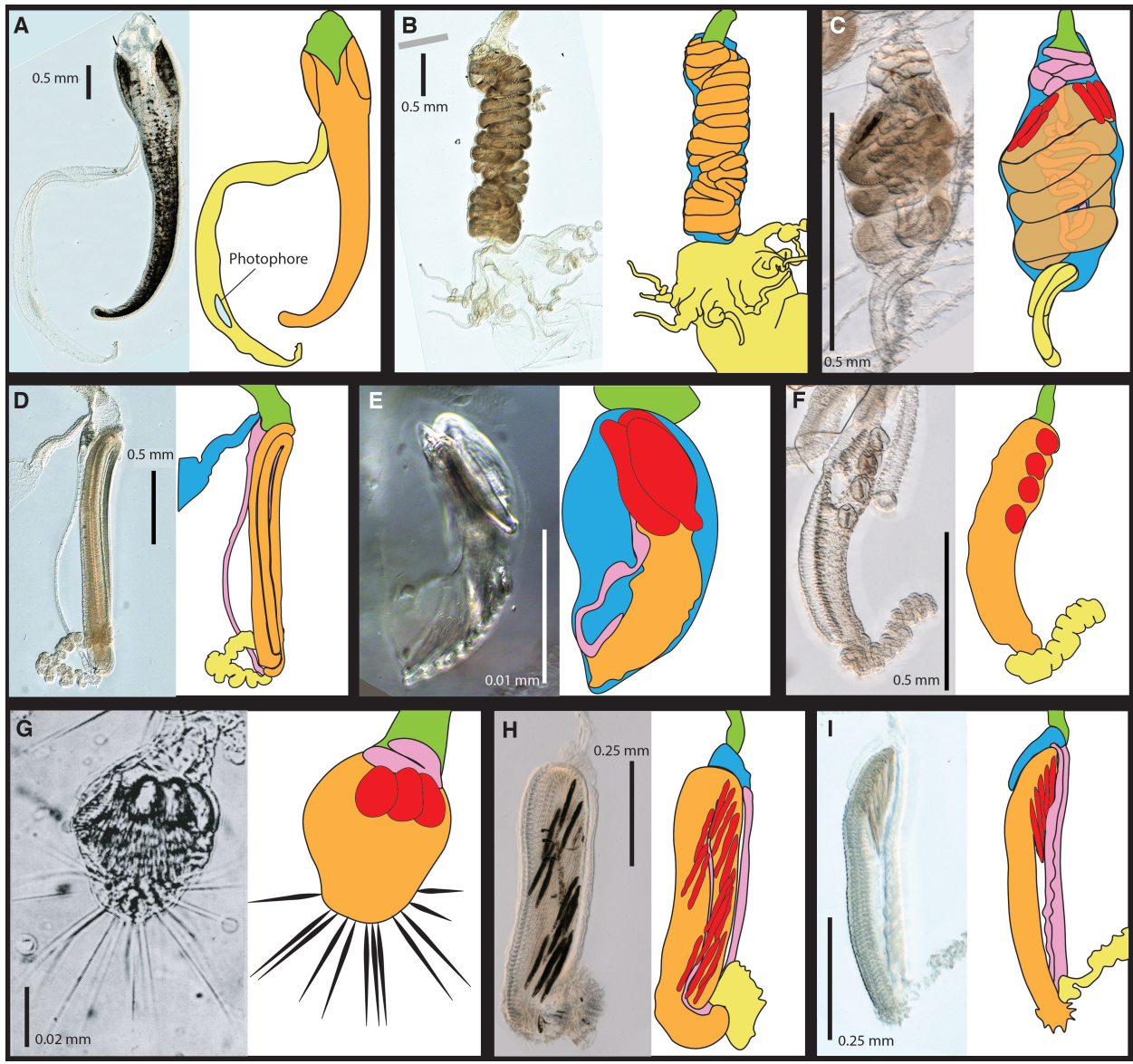


Figure 2: Tentillum diversity plate. The illustrations delineate the pedicle (green), involucrum (blue), cnidoband (orange), elastic strands (pink), terminal structures (yellow). Heteroneme nematocysts (stenoteles in C,E,F,G and mastigophores in H,I) are depicted in red for some species. A - *Erenna laciniata*, 10x. B - *Lychnagalma utricularia*, 10x. C - *Agalma elegans*, 10x. D - *Resomia ornicephala*, 10x. E - *Frillagalma vityazi*, 20x. F - *Bargmannia amoena*, 10x. G - *Cordagalma* sp., reproduced from Carré 1968. H - *Lilyopsis fluoracantha*, 20x. I - *Abylopsis tetragona*, 20x.

113 fieldwork expeditions, using blue-water diving (Haddock and Heine 2005), remotely operated
114 vehicles (ROVs), and human-operated submersibles. Tentacles were dissected from non-larval
115 gastrozooids, sequentially dehydrated into 100% ethanol, cleared in methyl salicylate, and
116 mounted onto slides with Canada Balsam or Permount mounting media. The slides were
117 imaged as tiled z-stacks using differential interference contrast (DIC) on an automated stage
118 at YPM-IZ (with the assistance of Daniel Drew and Eric Lazo-Wasem) and with laser point
119 confocal microscopy using a 488 nm Argon laser that excited autofluorescence in the tissues.
120 Thirty characters (defined in Appendix 2) were measured using Fiji (Collins 2007; Schindelin
121 et al. 2012). We did not measure the lengths of contractile structures (terminal filaments,
122 pedicles, gastrozooids, and tentacles), since they are too variable to quantify. We measured
123 at least one specimen for 96 different species (Appendix 3, Fig. 3). Of these, we selected 38
124 focal species across clades based on specimen availability and phylogenetic representation.
125 Three to five tentacle specimens from each one of these selected species were measured to
126 capture intraspecific variation.

127 In order to observe the discharge behavior of different tentilla, we recorded high speed
128 footage (1000-3000 fps) of tentillum and nematocyst discharge by live siphonophore specimens
129 (26 species) using a Phantom Miro 320S camera mounted on a stereoscopic microscope. We
130 mechanically elicited tentillum and nematocyst discharge using a fine metallic pin. We used
131 the Phantom PCC software to analyze the footage. For the 10 species recorded, we measured
132 total cnidoband discharge time (ms), heteroneme filament length (μm), and discharge speeds
133 (mm/s) for cnidoband, heteronemes, haplonemes, and heteroneme shafts when possible (data
134 in Appendix 4).

135 *Siphonophore phylogeny* – The phylogenetic analysis included 55 siphonophore species
136 and 6 outgroup cnidian species (*Clytia hemisphaerica*, *Hydra circumcincta*, *Ectopleura*
137 *dumortieri*, *Porpita porpita*, *Velella velella*, *Staurocladia wellingtoni*). The gene sequences
138 we used in this study are available online (accession numbers in Appendix 5). Some of
139 the sequences we used were accessioned in (Dunn et al. 2005), and others we extracted

from the transcriptomes in (Munro et al. 2018). Two new 16S sequences for *Frillagalma vityazi* (MK958598) and *Thermopalria* sp. (MK958599) sequenced by Lynne Christianson were included and accessioned to NCBI. We aligned these sequences using MAFFT (Katoh et al. 2002) (alignments available in Dryad). We inferred a Maximum Likelihood (ML) phylogeny (Appendix 6) from 16S and 18S ribosomal rRNA genes using IQTree (Nguyen et al. 2014) with 1000 bootstrap replicates (iqtree -s alignment.fa -nt AUTO -bb 1000). We used ModelFinder (Kalyaanamoorthy et al. 2017) implemented in IQTree v1.5.5. to assess relative model fit. ModelFinder selected GTR+R4 for having the lowest Bayesian Information Criterion score. Additionally, we inferred a Bayesian tree with each gene as an independent partition in RevBayes (Höhna et al. 2016) (Appendix 7 and 9), which was topologically congruent with the unconstrained ML tree. The *alpha* priors were selected to minimize prior load in site variation.

Given the broader sequence sampling of the transcriptome phylogeny, we ran constrained inferences (using both ML and Bayesian timetree approaches, which produced fully congruent topologies (Appendix 6 and 7)) after fixing the 5 nodes that were incongruent with the topology of the consensus tree in (Munro et al. 2018). This topology was then used to inform a Bayesian relaxed molecular clock time-tree in RevBayes, using a birth-death process (sampling probability calculated from the known number of described siphonophore species) to generate ultrametric branch lengths (Appendix 8). Scripts available in Appendix 9.

Feeding ecology – We extracted categorical diet data for different siphonophore species from published sources, including seminal papers (Biggs 1977; Purcell 1981, 1984; Andersen 1981; Mackie et al. 1987; Pugh and Youngbluth 1988; Bardi and Marques 2007), and ROV observation data (Hissmann 2005; Choy et al. 2017) with the assistance of Elizabeth Hetherington and C. Anela Choy (Appendix 10). We removed the gelatinous prey observations for *Praya dubia* eating a ctenophore and a hydromedusa, and for *Nanomia* sp. eating *Aegina*, since we believe these are rare events that have a much larger probability of being detected by ROV methods than their usual prey, and it is not clear whether the medusae were attempting to

167 prey upon the siphonophores. Personal observations on feeding (from SHDH, CAC, and Philip
168 Pugh) were also included for *Resomia ornicephala*, *Lychnagalma utricularia*, *Bargmannia*
169 *amoena*, *Erenna richardi*, *Erenna laciniata*, *Erenna sirena*, and *Apolemia rubriversa*. In order
170 to detect coarse-level patterns in the feeding habits, the data were merged into feeding guilds.
171 The feeding guilds described here are: small-crustacean specialist (feeding mainly on copepods
172 and ostracods), large crustacean specialist (feeding on large decapods, mysids, or krill), fish
173 specialist (feeding mainly on actinopterygian larvae, juveniles, or adults), gelatinous specialist
174 (feeding mainly on other siphonophores, medusae, ctenophores, salps, and/or doliolids), and
175 generalist (feeding on a combination of the aforementioned taxa, without favoring any one
176 prey group). These were selected to minimize the number of categories while keeping the
177 most different types of prey separate. We extracted copepod prey length data from (Purcell
178 1984). To calculate specific prey selectivities, we extracted quantitative diet and zooplankton
179 composition data from (Purcell 1981), matched each diet assessment to each prey field
180 quantification by site, calculated Ivlev's electivity indices (Jacobs 1974), and averaged those
181 by species (Appendix 11).

182 *Statistical analyses* – For subsequent comparative analyses, we removed species present in
183 the tree but not represented in the morphology data, and *vice versa*. Although we measured
184 specimens labeled as *Nanomia bijuga* and *Nanomia cara*, we are not confident in some of the
185 species-level identifications, and some specimens were missing diagnostic zooids. Thus, we
186 decided to collapse these into a single taxonomic concept (*Nanomia* sp.). All *Nanomia* sp.
187 observations were matched to the phylogenetic position of *Nanomia bijuga* in the tree. We
188 carried out all phylogenetic comparative statistical analyses in the programming environment
189 R (Team 2017), using the Bayesian ultrametric species tree (Fig. 4), and incorporating
190 intraspecific variation estimated from the specimen data as standard error whenever the
191 analysis tool allowed it (Appendix 3). R scripts available in Dryad. For each character (or
192 character pair) analyzed, we removed species with missing data and reported the number of
193 taxa included. We tested each character for normality using the Shapiro-Wilk test (Shapiro

¹⁹⁴ and Wilk 1965), and log-transformed those that were non-normal.

¹⁹⁵ We fitted different models generating the observed data distribution given the phylogeny
¹⁹⁶ for each continuous character using the function `fitContinuous` in the R package *geiger*
¹⁹⁷ (Harmon et al. 2007). The models compared were the white noise (WN; non-phylogenetic
¹⁹⁸ model that assumes all values come from a single normal distribution with no covariance
¹⁹⁹ structure among species), the Brownian Motion (BM) model of neutral divergent evolution
²⁰⁰ (Martins 1996), the Early Burst (EB) model of decreasing rate of evolutionary change (Harmon
²⁰¹ et al. 2010), and the Ornstein-Uhlenbeck (OU) model of stabilizing selection around a fitted
²⁰² optimum state (Uhlenbeck and Ornstein 1930; Butler and King 2004). We then ranked the
²⁰³ models in order of increasing parametric complexity (WN,BM,EB,OU), and compared the
²⁰⁴ corrected Akaike Information Criterion (AICc) support scores (Sugiura 1978) to the lowest
²⁰⁵ (best) score, using a cutoff of 2 units to determine significantly better support. When the
²⁰⁶ best fitting model was not significantly better than a less complex alternative, we selected
²⁰⁷ the least complex model (Appendix 12). We calculated model adequacy scores using the
²⁰⁸ R package *arbutus* (Pennell et al. 2015) (Appendix 13). We calculated phylogenetic signal
²⁰⁹ in each of the measured characters using Blomberg's K (Blomberg et al. 2003) (Appendix
²¹⁰ 12). We reconstructed ancestral states using Maximum Likelihood (R `phytools::anc.ML`
²¹¹ (Revell 2012)), and stochastic character mapping (R `phytools::make.simmap`) for categorical
²¹² characters. R scripts available in Dryad.

²¹³ In order to study the evolution of predatory specialization, we reconstructed components
²¹⁴ of the diet and prey selectivity on the phylogeny using ML (R `phytools::anc.ML`). To identify
²¹⁵ evolutionary associations of diet with tentillum and nematocyst characters, we compared the
²¹⁶ performance of a neutral evolution model to that of a diet-driven directional selection model.
²¹⁷ First, we collapsed the diet data into the five feeding guilds mentioned above (fish specialist,
²¹⁸ small crustacean specialist, large crustacean specialist, gelatinous specialist, generalist), based
²¹⁹ on which prey types they were observed consuming most frequently. Then, we reconstructed
²²⁰ the feeding guild ancestral states using the ML function `ace` (package *ape* (Paradis et al.

221 2019)), removing tips with no feeding data. The ML reconstruction was congruent with the
222 consensus stochastic character mapping (Appendix 18). Then, using the package *OUwie*
223 (Beaulieu and O'Meara 2012), we fitted an OU model with multiple optima and rates of
224 evolution matched to the reconstructed ancestral diet regimes, a single optimum OU model,
225 and a BM null model, inspired by the analyses in (Cressler et al. 2015). Finally, we compared
226 their AICc support values to select the best fitting model (Appendix 14).

227 To model the evolutionary associations between individual tentillum and nematocyst
228 characters and the ability to capture particular prey types in the diet, we ran a series of
229 phylogenetic generalized linear models (R `phyloglm::phyloglm`) (Appendix 17). In addition,
230 we ran a series of comparative analyses to address hypotheses of diet-tentillum relationships
231 posed in the literature. To test for correlated evolution among binary characters, we used
232 Pagel's test (Pagel 1994). To characterize and evaluate the relationship between continuous
233 characters, we used phylogenetic generalized least squares regressions (PGLS) (Grafen 1989).
234 To compare the evolution of continuous characters with categorical aspects of the diet, we
235 carried out a phylogenetic logistic regression (R `nlme::gls` using the 'corBrownian' function
236 for the argument 'correlation').

237 To generate hypotheses about the diets of understudied siphonophores for which no feeding
238 observations have yet been reported (but for which we have tentacle morphology data), we
239 carried out linear discriminant analysis of principal components (DAPC) using the `dapc`
240 function (R `adegenet::dapc`) (Jombart et al. 2010). This function allowed us to incorporate
241 more predictors than individuals. We generated discriminant functions for feeding guild,
242 soft/hard bodied prey, and for the presence of copepods, fish, and shrimp (large crustaceans) in
243 the diet (Appendix 15). Some taxa have inapplicable states for certain absent characters (such
244 as the length of a nematocyst subtype that is not present in a species), which are problematic
245 for DAPC analyses. We tackled this by transforming the absent states to zeroes. This
246 approach allows us to incorporate all the data, but creates an attraction bias between small
247 character states (*e.g.* small tentilla) and absent states (*e.g.* no tentilla). Absent characters are

likely to be very biologically relevant to prey capture and we believe they should be accounted for in a predictive approach. We limited the number of linear discriminant functions retained to the number of groupings in each case. We selected the number of principal components retained using the a-score optimization function (R `adegenet::optim.a.score`) (Jombart et al. 2010) with 100 iterations, which yielded more stable results than the cross validation function (R `adegenet::xval`). This optimization aims to find the compromise value with highest discrimination power with the least overfitting. From these DAPCs we obtained the highest contributing morphological characters to the discriminaton (characters in the top quartile of the weighted sum of the linear discriminant loadings controlling for the eigenvalue of each discriminant). For each DAPC we generated hypotheses about the diets of siphonophores outside the training set (R `adegenet::predict.dapc`), incorporating prediction uncertainty as posterior probabilities (Appendix 15). In order to identify the sign of the relationship between the predictor characters prey type presence in the diet, we then generated generalized logistic regression models (as a type of generalized linear model, or GLM using R `stats::glm`) with the top contributing characters (from the corresponding DAPC) as predictors. We also carried out these GLMs on the Ivlev's selectivity indices for each prey type calculated from (Purcell 1981) (in Appendix 11).

In order to explore the correlational structure among continuous characters and among their evolutionary histories, we used principal component analysis (PCA) and phylogenetic PCA (Revell 2012). Since the character dataset contains many gaps due to missing characters and inapplicable states, we carried out these analyses on a subset of species and characters that allowed for the most complete dataset. This was done by removing the terminal filament characters (which are only shared by a small subset of species), and then removing species which had inapplicable states for the remaining characters. In addition, we obtained the correlations between the phylogenetic independent contrasts (Felsenstein 1985) using the package rphylip (Revell and Chamberlain 2014).

In order to study correlations between the rates of evolution between different characters,

275 we fitted a set of evolutionary variance covariance matrices (Revell and Collar 2009) (R
276 phytools::evol.vcv). When fitting all covariance terms simultaneously (Appendix 20.1-20.3),
277 we selected the largest set of characters that would allow the analysis to run without
278 computational singularities. This excluded many of the morphometric characters which are
279 linearly dependent on other characters. Since the functions do not tolerate missing data,
280 we ran the analyses in two ways: One including all taxa but transforming absent states
281 to zeroes, and another removing the taxa with absent states. To test whether phenotypic
282 integration changes across selective regimes determined by the reconstructed feeding guilds,
283 we carried out character-pairwise variance covariance analysis comparing alternative models
284 (R phytools::evolvcv.lite), including those where correlations are the same across the whole
285 tree and models where correlations differ between selective regimes. These analyses could
286 only be carried out on the subset of taxa for which diet data is available, and only among
287 character pairs that are not computationally singular for that taxonomic subset. Finally, we
288 compared regime-specific variance covariance matrices to the general matrix and to their
289 preceding regime matrix to identify the changes in character dependence unique to each
290 regime (see Appendix 20). Gelatinous specialist correlations could only be estimated for a
291 small subset of characters present in *Apolemia*, and should be interpreted with care.

292 To test how many times extreme nematocyst morphologies evolved, we reconstructed
293 the ancestral states of $\log(\text{length}/\text{width})$ of the different cnidoband nematocyst types, and
294 identified the branches with the greatest shifts. In addition to characterizing the shifts in the
295 state values of haploneme and heteroneme elongation, we identified and located regime shifts
296 for the rate of evolution using a Bayesian Analysis of Macroevolutionary Mixtures (BAMM)
297 (Rabosky et al. 2014) (Appendix 16).

298 Results

299 *Phylogeny* – Only 5 nodes (blue dots in Figure 4) in the unconstrained inference were
300 incongruent with the (Munro et al. 2018) transcriptome tree, and these were constrained

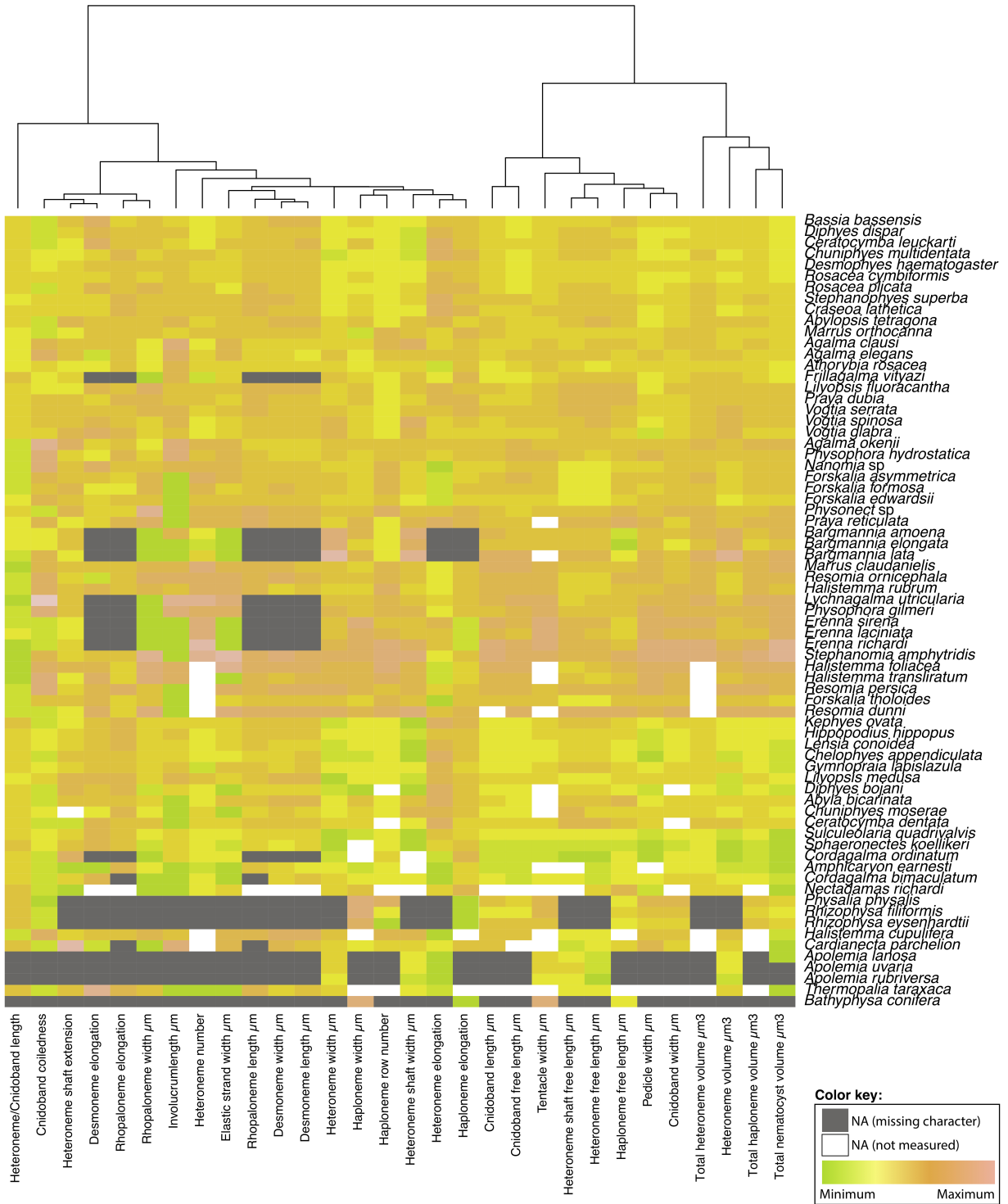


Figure 3: Heatmap summarizing the morphological diversity measured for 96 species of siphonophores clustered by similarity (raw data in Appendix 3). Missing values from absent characters presented as dark grey cells, missing values produced from technical difficulties presented as white cells. Values scaled by character.

³⁰¹ during estimation of the 18S+16S tree. The topology of the constrained tree presented here
³⁰² (Fig. 4) is congruent with the resolved nodes in (Dunn et al. 2005) and (Munro et al. 2018).

³⁰³ We retained the clade nomenclature defined in (Dunn et al. 2005) and (Munro et al.
³⁰⁴ 2018), such as Codonophora to indicate the sister group to Cystonectae, Euphysonectae to
³⁰⁵ indicate the sister group to Calycophorae, Clade A and B to indicate the two main lineages
³⁰⁶ within Euphysonectae. In addition, we define two new clades within Codonophora (Fig. 4):
³⁰⁷ Eucladophora as the clade containing *Agalma elegans* and all taxa that are more closely related
³⁰⁸ to it than to *Apolemia lanosa*, and Tendiculophora as the clade containing *Agalma elegans* and
³⁰⁹ all taxa more closely related to it than to *Bargmannia elongata*. Eucladophora is characterized
³¹⁰ by bearing spatially differentiated tentilla with proximal heteronemes and a narrower terminal
³¹¹ filament region. The etymology derives from the Greek *eu+kládos+phóros* for “true branch
³¹² bearers”. Tendiculophora are characterized by bearing rhopalonemes and desmonemes in the
³¹³ terminal filament, having a pair of elastic strands, and developing proximally detachable
³¹⁴ cnidobands. The etymology of this clade is derived from the Latin *tendicula* for “snare or
³¹⁵ noose” and the Greek *phóros* for “carriers”.

³¹⁶ *Evolutionary dynamics between diet and tentillum morphology* – Reconstructions of feeding
³¹⁷ guilds shows that generalism is not likely to be ancestral, and it appears to have evolved at
³¹⁸ least two times independently (Fig. 5). Large crustacean specialists evolve into generalists
³¹⁹ twice independently, supporting hypothesis 3. Feeding guild specializations have shifted
³²⁰ from an alternative ancestral state at least five times, supporting hypothesis 2. Copepod
³²¹ specialization and fish specialization evolved twice, and ostracod specialization evolved at
³²² least once.

³²³ The OUwie model comparison shows that out of 30 characters, 10 show significantly
³²⁴ stronger support for the diet-driven multi-optima multi-rate OU model (Appendix 14). These
³²⁵ characters include terminal filament nematocyst size and shape, involucrum length, elastic
³²⁶ strand width, and heteroneme number. Most of these characters are found exclusively in
³²⁷ Tendiculophora, thus this may reflect processes that could be unique to this subtree. Five

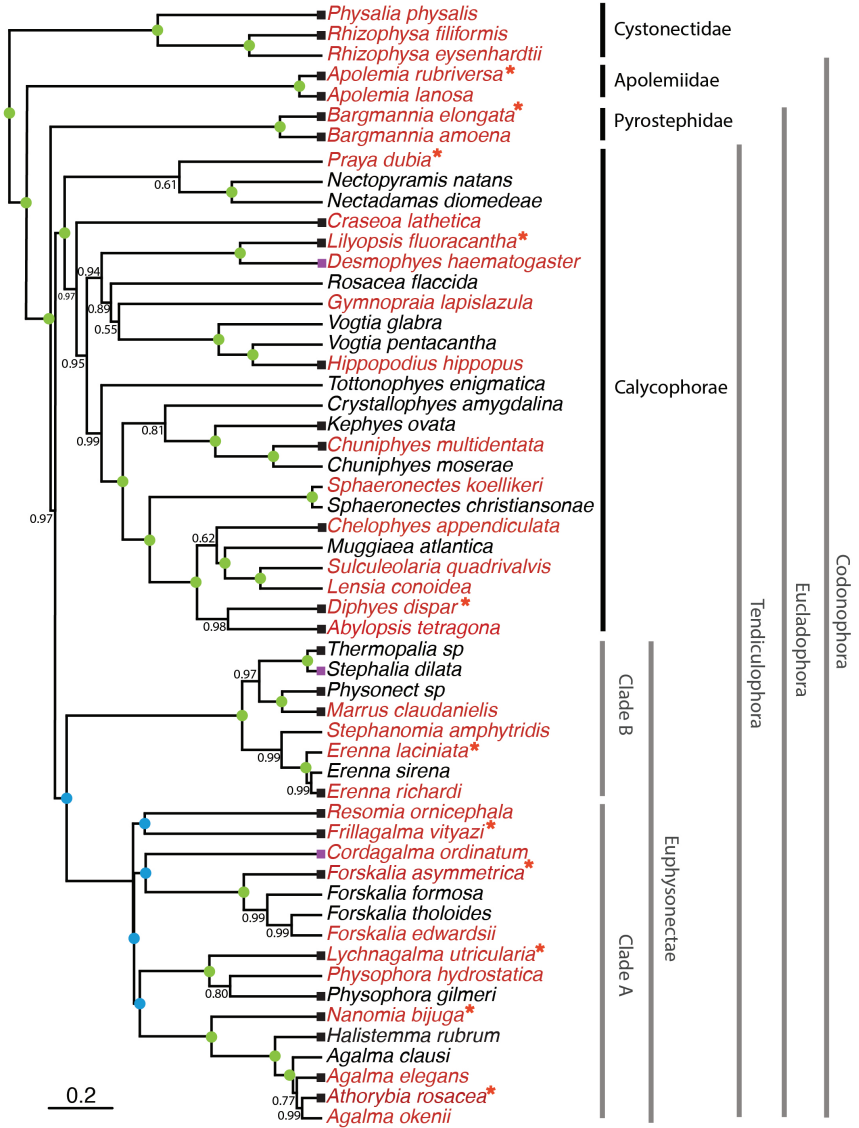


Figure 4: Bayesian time-tree built from 18S + 16S concatenated sequences. Branch lengths estimated using relaxed molecular clock. Species names in red indicate replicated representation in the morphology data. Species marked with an asterisk were recorded using high speed video. Nodes labeled with bayesian posteriors (BP). Green circles indicate BP = 1. Blue circles indicate nodes constrained to be congruent with (Munro *et al.* 2018). Tips with black squares indicate the species with transcriptomes used in (Munro *et al.* 2018). Tips with grey squares indicate genus-level correspondence to taxa included in (Munro *et al.* 2018). The main clades are labeled: in black for described taxonomic units, and in grey for operational phylogenetic designations.

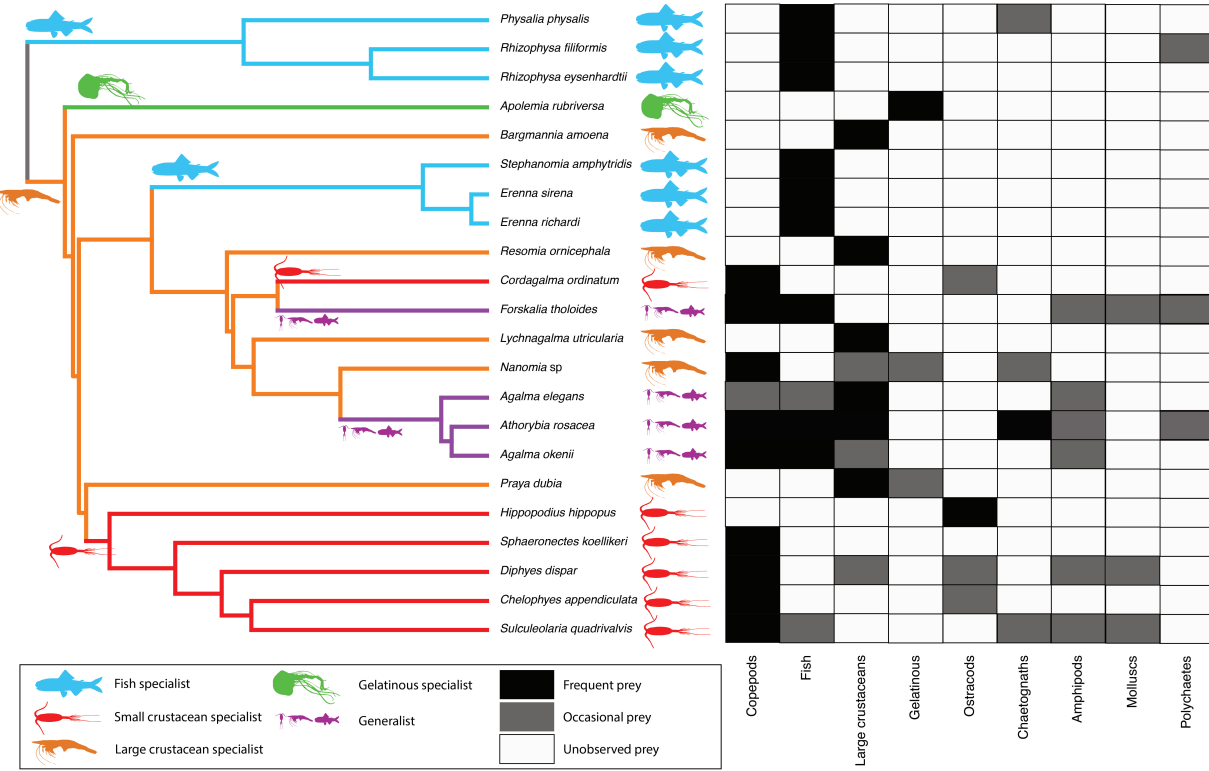


Figure 5: Left - Subset phylogeny showing the mapped feeding guild regimes that were used to inform the *OUwie* analyses. Right - Grid showing the prey items consumed from which the feeding guild categories were derived. Diet data were obtained from the literature review in Appendix 10.

328 characters including cnidoband length, cnidoband shape, and haploneme length show maximal
 329 support for a diet-driven single-optimum OU model. The remaining 15 characters support
 330 BM (or OU with marginal AICc difference with BM).

331 Phylogenetic logistic regressions identified evolutionary associations between individual
 332 characters and the presence of particular prey types in the diet (Fig. 5, right). Shifts toward
 333 ostracod presence in diet correlated with reductions in pedicle width and total haploneme
 334 volume. Shifts to copepod presence in the diet were associated with reductions in haploneme
 335 width, cnidoband length and width, total haploneme and heteroneme volumes, and tentacle
 336 and pedicle widths. Consistently, transitions to decapod presence in the diet correlated with
 337 more coiled cnidobands (Appendix 17).

338 Phylogenetic regressions of continuous characters against prey selectivity data produced

additional insights. Fish selectivity is associated with increased number of heteronemes per tentillum, increased roundness of nematocysts (desmonemes and haplonemes), larger heteronemes, reduced heteroneme/cnidoband length ratios, smaller rhopalonemes, lower haploneme SA/V ratios, and increased size of the cnidoband, elastic strand, pedicle and tentacle widths. Decapod-selective diets were associated with increasing cnidoband size and coiledness, haploneme row number, elastic strand width, and heteroneme number. Copepod-selective diets evolved in association with smaller heteroneme and total nematocyst volumes, smaller cnidobands, rounder rhopalonemes, elongated heteronemes, narrower haplonemes with higher SA/V ratios, and smaller heteronemes, tentacles, pedicles and elastic strands. Selectivity for ostracods was associated with reductions in size and number of heteroneme nematocysts, reductions in cnidoband size, number of haploneme rows, heteroneme number, and cnidoband coiledness. Heteroneme length and elongation also correlated negatively with chaetognath selectivity.

When some of the diet-morphology associations reported in the literature (Purcell 1984; Purcell and Mills 1988) were tested for correlated evolution (Table 1), we found that most were consistent with an evolutionary explanation except the relationship between terminal filament nematocysts (rhopalonemes and desmonemes) and crustaceans in the diet. The latter is likely a product of the larger species richness of crustacean-eating species with terminal filament nematocysts, rather than simultaneous evolutionary gains.

Table 1. Tests of correlated evolution between morphological characters and aspects of the diet found correlated in the literature.

Character	Aspect of diet	Test of evolutionary association	Relationship sign	P-value	Number of taxa	Association first report
Differentiated cnidobands	Hard bodied prey	Page's test	+	0.017	19	Purcell, 1984
Heteroneme volume	Copepod prey size	pGLS	+	0.002	8	Purcell, 1984
Terminal filament nematocysts	Crustacean diet	Page's test	Non-Significant	0.200	19	Purcell & Mills, 1988
Number of nematocyst types	Soft-bodied prey	Phylogenetic logistic regression	-	0.040	22	Purcell & Mills, 1988

360

361

Generating dietary hypotheses using tentillum morphology – The discriminant analysis of principal components for feeding guild (7 principal components, 4 discriminants) produced

364 100% discrimination, and the highest loading contributions were found for the characters
 365 (ordered from highest to lowest): Involucrum length, heteroneme volume, heteroneme number,
 366 total heteroneme volume, tentacle width, heteroneme length, total nematocyst volume, and
 367 heteroneme width (Appendix 15.1). We used the predictions from this discriminant function
 368 to generate hypotheses about the feeding guild of 45 species in our morphological data (Fig.
 369 @figure6)). This projection predicts that two other *Apolemia* species may also be gelatinous
 370 prey specialists like *Apolemia rubriversa*, and that *Erenna laciniata* may be a fish specialist
 371 like *Erenna richardi*.

372 Table 2. Discriminant analysis of principal components for the presence of specific prey
 373 types using the morphological data. Top quartile variable (character) contributions to the
 374 linear discriminants are ordered from highest to lowest. Logistic regressions and GLMs were
 375 fitted to predict prey type presence and selectivity respectively. The sign of the slope of
 376 each predictor is reported, marked with an asterisk if significant, and highlighted grey if it
 377 differs between prey presence in diet and prey selectivity. green if significant (p value < 0.05).
 378 Pseudo-R² (%) approximates the percent variance explained by the model.

Prey type	Discrimination (%)	DAPC		GLM for prey type presence (22 taxa)		Best fitting GLM for prey type selectivity (Purcell, 1981) (7 taxa)	
		Top quartile variable contributions	Sign	Pseudo-R ² (%)	Sign	Pseudo-R ² (%)	
Copepods	95.4	Total nematocyst volume	-		-*		
		Tentacle width	-		+		
		Haploneme elongation	-		+		
		Haploneme surface area/volume ratio	+	67.8	-		
		Haploneme row number	+		+		
		Cnidoband length	-		+		
		Cnidoband width	-		-		
Fish	68.1	Cnidoband free length	+		+		
		Total haploneme volume	-		+		
		Heteroneme volume	+		-		
		Total nematocyst volume	-		+		
		Total heteroneme volume	-	45.8	-		
		Cnidoband length	-		-		
		Cnidoband free length	+		+		
Large crustaceans	81.8	Involucrum length	-		-		
		Pedicle width	+		+		
		Involucrum length	++*		+		
		Total heteroneme volume	-		-		
		Elastic strand width	-		++*		
		Rhopaloneme length	+	73.2	+		
		Heteroneme volume	+		-		

379

When predicting soft- and hard-bodied prey specialization, the DAPC achieved 90.9% discrimination success, only marginally confounding hard-bodied specialists with generalists (Appendix 15.4). The main characters driving this discrimination are involucrum length, heteroneme number, heteroneme volume, tentacle width, total nematocyst volume, total haploneme volume, elastic strand width, and heteroneme length. Discriminant analyses and GLM logistic regressions were also applied to specific prey type presence and selectivity (Table 2), revealing the sign of their predictive relationship to each prey type. We only selected prey types with sufficient variation in the data to carry out these analyses (copepods, fish, and large crustaceans). While the presence of fish or large crustaceans in the diet cannot be unambiguously discriminated using tentillum morphology (Appendix 15), specialization on fish or large crustacean prey can be fully disentangled (Appendix 15.1). For each prey type studied, tentillum morphology is a much better predictor of prey selectivity than of prey presence in the diet, despite prey selectivity data being available for a smaller subset of species. Interestingly, many of the morphological predictors had opposite slope signs when predicting prey selectivity *versus* predicting prey presence in the diet (Table 2).

Evolution of tentillum and nematocyst characters – One third of the characters measured support a non-phylogenetic generative model, indicating they are not phylogenetically conserved (Appendix 12). Total nematocyst volume and cnidoband-to-heteroneme length ratio showed strongly conserved phylogenetic signals. 74% of characters present a significant phylogenetic signal, yet only total nematocyst volume, haploneme length, and heteroneme-to-cnidoband length ratio had a phylogenetic signal with $K > 1$. 67% of characters support BM models, indicating a history of neutral constant divergence. No relationship between phylogenetic signal and BM model support was found. Haploneme nematocyst length is the only character with support for an EB model of decreasing rate of evolution with time. No character had support for a single-optimum OU model (when uninformed by feeding guild regime priors).

The phylogenetic positions of the main categorical character shifts were reconstructed



Figure 6: Hypothetical feeding guilds for siphonophore species predicted by a 6 PCA DAPC (in Appendix 15.1). Cell darkness indicates posterior probability of belonging to each guild. Training data set transformed so inapplicable states are computed as zeroes. Species ordered and colored according to their predicted feeding guild.

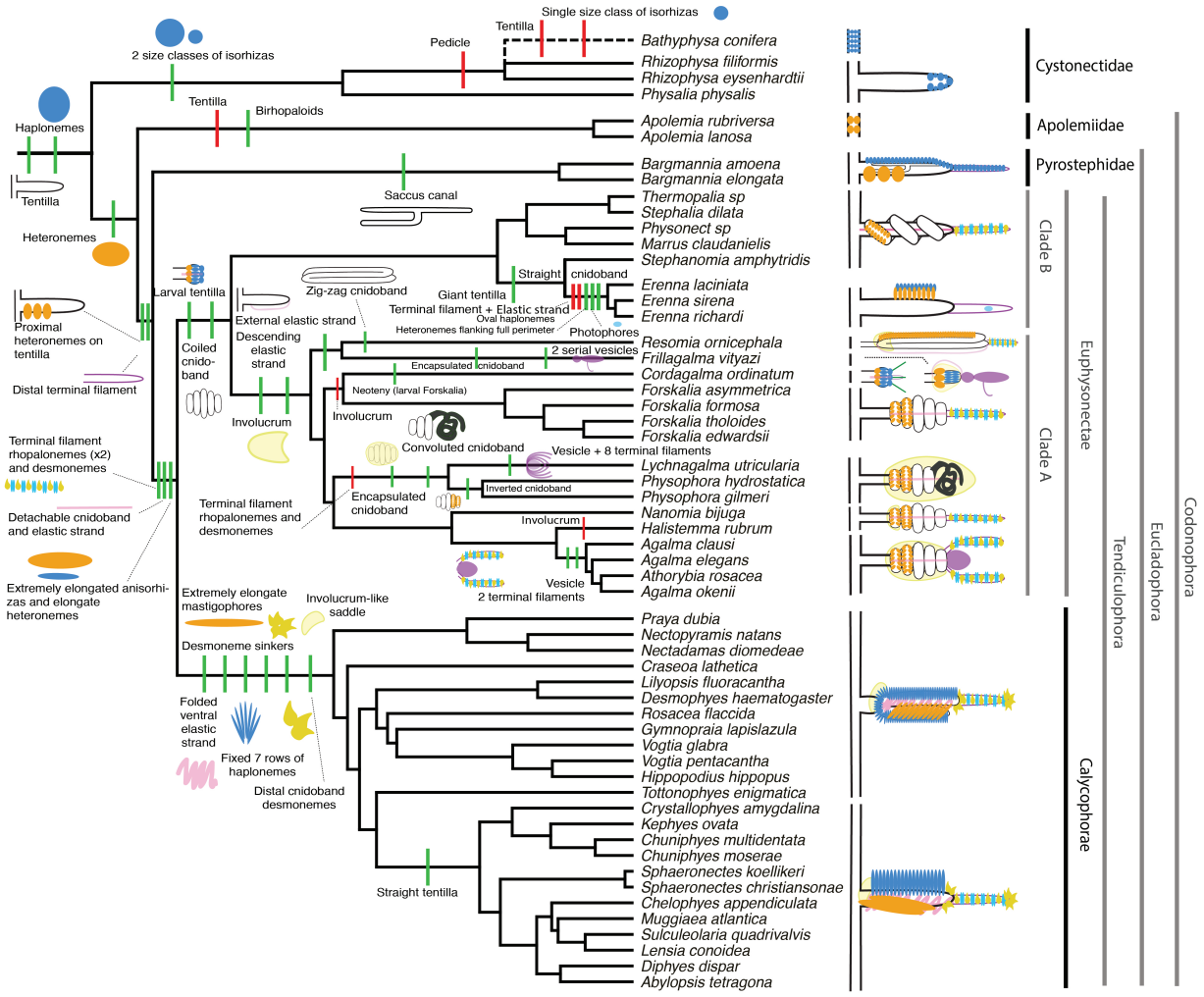


Figure 7: Siphonophore cladogram with the main categorical character gains (green) and losses (red) mapped. Some branch lengths were modified from the Bayesian chronogram to improve readability. The main visually distinguishable tentillum types are sketched next to the species that bear them, showing the location and arrangement of the main characters. In large, complex-shaped euphysonect tentilla, haplonemes were omitted for simplification. The rhizophysid *Bathypysa conifera* branch was appended manually as a polytomy (dashed line).

407 using stochastic character mapping (Appendix 18), and summarized in Figure 7. Haploneme
408 nematocysts are likely ancestrally present in siphonophore tentacles, since they are present in
409 the tentacles of many other hydrozoans. Haplonemes first diverged into spherical isorhizas
410 of 2 size classes in Cystonectae, and elongated anisorhizas of one size class in Codonophora.
411 Haplonemes were likely lost in the tentacles of *Apolemia*, but spherical isorhizas are retained in
412 other *Apolemia* tissues (Siebert et al. 2013). Similarly, while heteronemes exist in other tissues
413 of cystonects, they appear in the tentacles of codonophorans exclusively, as birhopaloids in
414 *Apolemia*, ancestral stenoteles in eucladophoran physonects, and microbasic mastigophores in
415 calycophorans.

416 Eucladophora (the clade containing Pyrostephidae, Euphysonectae, and Calycophorae,
417 see Fig. 4) encompasses most of the extant Siphonophore species (178 of 186) other than
418 Cystonects and *Apolemia*. Innovations evolved in the stem of this group include spatially
419 segregated heteroneme and haploneme nematocysts, terminal filaments, and elastic strands
420 (Fig. 7). Pyrostephids evolved a unique bifurcation of the axial gastrovascular canal of
421 the tentillum known as the “saccus” (Totton and Bargmann 1965). The stem to the clade
422 Tendiculophora (clade containing Euphysonectae and Calycophorae, see Fig. 4) subsequently
423 acquired further novelties such as the desmoneme and rhopaloneme (acrophore subtype
424 ancestral) nematocysts on the terminal filament (Fig. 7), which bears no other nematocyst
425 type (Fig. 1). These are arranged in sets of 2 parallel rhopalonemes for each single desmoneme
426 (Skaer 1988, 1991). The involucrum is an expansion of the epidermal layer that can cover part
427 or all of the cnidoband (Fig. 2). This structure, together with differentiated larval tentilla,
428 appeared in the stem branch to Clade A physonects. Calycophorans evolved novelties such as
429 larger desmonemes at the distal end of the cnidoband, pleated pedicles with a “hood” (here
430 considered homologous to the involucrum) at the proximal end of the tentillum, anacrophore
431 rhopalonemes, and microbasic mastigophore-type heteronemes. While calycophorans have
432 diversified into most of the extant described siphonophore species (108 of 186), their tentilla
433 have not undergone any major categorical gains or losses since their most recent common

434 ancestor. Nonetheless, they have spread over a broad span of variation in nematocyst and
435 cnidoband sizes.

436 *Phenotypic integration of the tentillum* – The quantitative characters we measured from
437 tentilla and their nematocysts are highly correlated. The results indicate that the dimen-
438 sionality of tentillum morphology is low, that many traits are associated with size, but that
439 nematocyst arrangement and shape are independent of it. Of the phylogenetic correlations
440 (Fig. 8a, lower triangle), 81.3% were positive and 18.7% were negative, while of the ordinary
441 correlations (Fig. 8a, upper triangle) 74.6% were positive and 25.4% were negative. Half
442 (49.9%) of phylogenetic correlations were >0.5 , while only 3.6% are < -0.5 . Similarly, of the
443 across-species correlations, 49.1% were >0.5 and only 1.5% were < -0.5 . We found that 13.9%
444 of character pairs had opposing phylogenetic and ordinary correlation coefficients. Just 4%
445 have negative phylogenetic and positive ordinary correlations (such as rhopaloneme elongation
446 \sim heteroneme-to-cnidoband length ratio and haploneme elongation, or haploneme elongation
447 \sim heteroneme number), and only 9.9% of character pairs had positive phylogenetic correlation
448 yet negative ordinary correlation (such as heteroneme elongation \sim cnidoband convolution
449 and involucrum length, or rhopaloneme elongation with cnidoband length). These disparities
450 can be caused by Simpson's paradox (Blyth 1972): the reversal of the sign of a relationship
451 when a third variable (or a phylogenetic topology (Uyeda et al. 2018)) is considered. However,
452 no character pair had correlation coefficient differences larger than 0.64 between ordinary
453 and phylogenetic correlations (heteroneme shaft extension \sim rhopaloneme elongation has a
454 Pearson's correlation of 0.10 and a phylogenetic correlation of -0.54). Rhopaloneme elongation
455 shows the most incongruencies between phylogenetic and ordinary correlations with other
456 characters.

457 The variance covariance matrices (Appendix 20.1-20.2) are congruent with the abundant
458 positive correlations observed among simple measurement characters in Fig. 8a. However,
459 this analysis reveals more clearly the diagonal blocks that constitute the evolutionary modules,
460 such as the heteroneme block, the terminal filament nematocyst block, and the cnidoband-

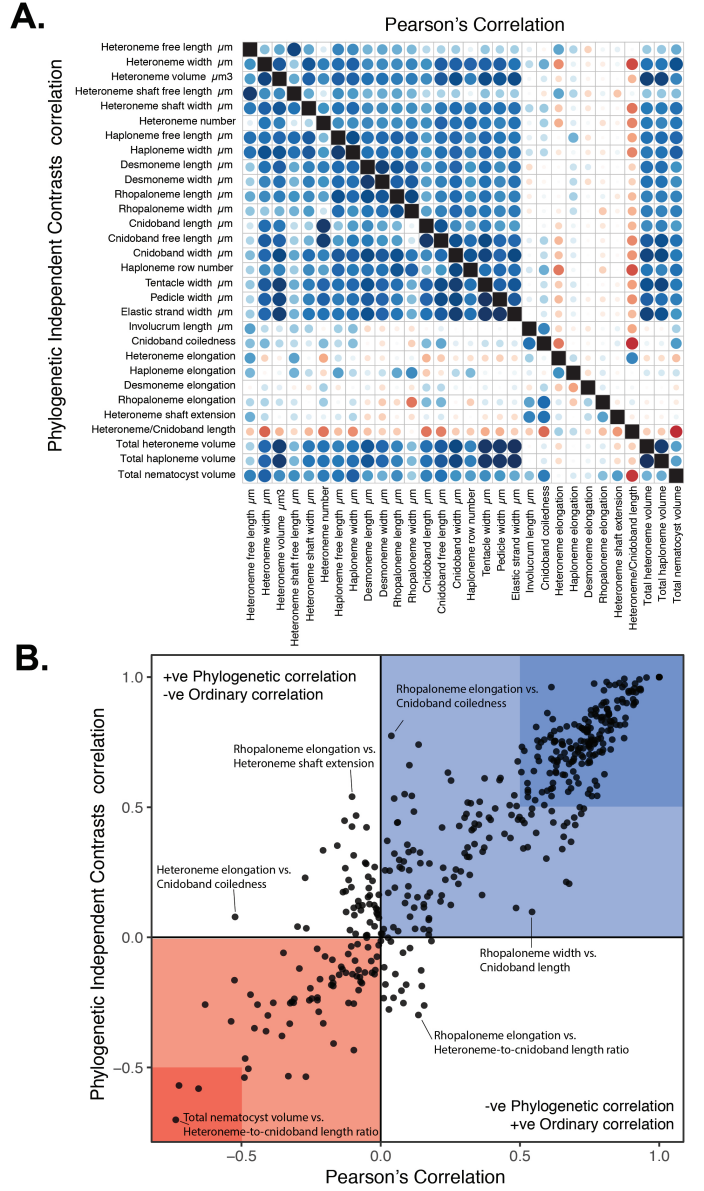


Figure 8: A. Correlogram showing strength of ordinary (upper triangle) and phylogenetic (lower triangle) correlations between characters. Both size and color of the circles indicate the strength of the correlation (R^2). B. Scatterplot of phylogenetic correlation against ordinary correlation showing a strong linear relationship ($R^2 = 0.92$, 95% confidence between 0.90 and 0.93). Light red and blue boxes indicate congruent negative and positive correlations respectively. Darker red and blue boxes indicate strong (<-0.5 or >0.5) negative and positive correlation coefficients respectively.

⁴⁶¹ pedicle-tentacle block. These results were not very sensitive to transformation of inapplicable
⁴⁶² states and taxon sampling. When we compared the rate covariance terms between characters
⁴⁶³ across the different feeding guild regimes (Appendix 20.4), we found that half (48%) of the
⁴⁶⁴ character pairs presented distinct correlation coefficients across different regimes, indicating
⁴⁶⁵ that the mode of phenotypic integration may also shift with trophic niche. When contrasting
⁴⁶⁶ the regime-specific rate correlation matrices to the whole-tree matrix, we were able to identify
⁴⁶⁷ the character dependencies that are unique to each predatory niche (Appendix 20.6).

⁴⁶⁸ Under the majority of SIMMAP outcomes, large crustaceans specialists are the first regime
⁴⁶⁹ to appear, and other regimes evolve in a shift from this ancestral specialization. Compared
⁴⁷⁰ to the rate correlation matrix estimated over the whole tree, large crustacean specialists
⁴⁷¹ present strong negative correlations between haploneme elongation and heteroneme size,
⁴⁷² and between rhopaloneme elongation and tentillum size, as well as with involucrum length.
⁴⁷³ With the appearance of generalists (*Forskalia* and the *Agalma-Athorybia* clade), terminal
⁴⁷⁴ filament nematocyst (desmonemes and rhopalonemes) sizes became negatively correlated with
⁴⁷⁵ the sizes of most characters, meaning that as some tentilla became larger, their individual
⁴⁷⁶ terminal nematocysts became smaller, observed to the extreme in *Agalma*. In addition,
⁴⁷⁷ heteroneme and rhopaloneme elongation became positively correlated with cnidoband size.
⁴⁷⁸ When large crustacean specialists switched to small crustacean prey in *Cordagalma* and
⁴⁷⁹ calycophorans, haploneme size became inversely correlated with heteroneme elongation,
⁴⁸⁰ which in turn developed a strong positive relationship with tentillum size. In other words, as
⁴⁸¹ tentilla get smaller in this group, heteronemes get shorter and haplonemes get larger. The
⁴⁸² extremes of this gradient can be seen in *Cordagalma* and *Hippopodius*. With the evolution
⁴⁸³ of fish prey specialization in cystonects and within Clade B, haploneme elongation became
⁴⁸⁴ negatively correlated with heteroneme elongation (signal driven by Clade B, since cystonects
⁴⁸⁵ lack tentacular heteronemes), and the surface area to volume ratio of haploneme nematocysts
⁴⁸⁶ switched from a strong negative relationship with cnidoband size (found in every other
⁴⁸⁷ regime) to a positively correlation. Gelatinous specialization, albeit appearing only once in

488 our tree, also carries a unique signature in character rate correlation shifts, with an increase
489 in the strength of the correlation between heteroneme shape and shaft width, consistent with
490 the appearance of birrhopaloid nematocysts with swollen shafts that are likely effective at
491 anchoring gelatinous tissue (see reference to Narcomedusae nematocysts in (Purcell and Mills
492 1988)).

493 In the non-phylogenetic PCA morphospace using only simple characters (Fig. 9), PC1
494 (aligned with tentillum and tentacle size) explained 69.3% of the variation in the tentillum
495 morphospace, whereas PC2 (aligned with heteroneme length, heteroneme number, and
496 haploneme arrangement) explained 13.5%. In a phylogenetic PCA, 63% of the evolutionary
497 variation in the morphospace is explained by PC1 (aligned with shifts in tentillum size), while
498 18% is explained by PC2 (aligned with shifts in heteroneme number and involucrum length).

499 *Evolution of nematocyst shape* – Haploneme nematocyst evolution has been mainly driven
500 by a single large shift towards elongation in Tendiculophora, which contains the majority of
501 described siphonophore species other than Cystonects, *Apolemia*, and Pyrostephidae. There
502 is one secondary return to more oval, less elongated haplonemes in *Erenna*, but it does not
503 reach the sphericity present in Cystonectae or Pyrostephidae (Fig. 10). Heteroneme evolution
504 presents a less discrete evolutionary history, where Tendiculophora evolved more elongate
505 heteronemes, but the difference between theirs and other siphonophores is much smaller than
506 the variation in shape within Tendiculophora, bearing no phylogenetic signal. In this clade,
507 evolution of heteroneme shape has diverged in both directions, and there is no correlation
508 with haploneme shape (Fig. 10), which has remained fairly constant (elongation between 1.5
509 and 2.5).

510 Haploneme and heteroneme shape share 21% of their variance across extant values, and
511 53% of variance in their shifts along the branches of the phylogeny. However, much of this
512 correlation is due to the contrast between Pyrostephidae and their sister group Tendiculophora
513 (Fig. 4). BAMM identified a regime shift in heteroneme shape evolution on the branches
514 leading to *Agalma* and *Athorybia*. For the rates of haploneme shape evolution, BAMM

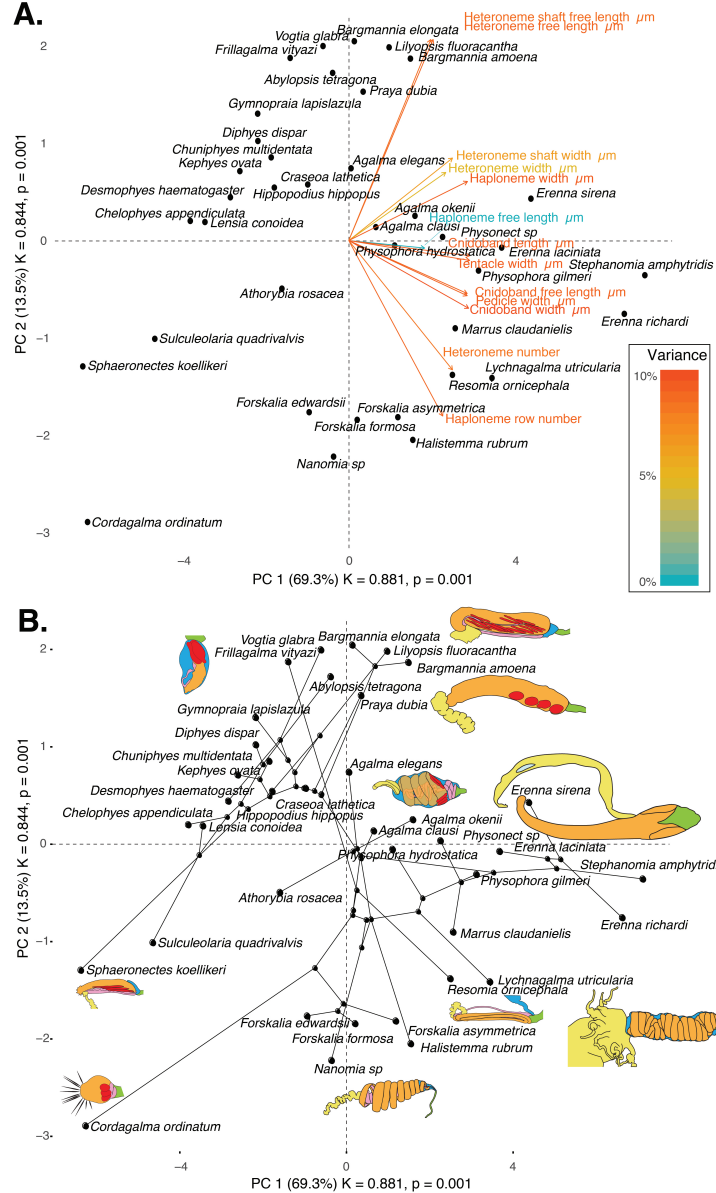


Figure 9: Phylomorphospace of the simple continuous characters principal components, excluding ratios and composite characters. A. Variance explained by each variable in the PC1-PC2 plane. Axis labels include the phylogenetic signal (K) for each component and p-value. B. Phylogenetic relationships between the species points distributed in that same space.

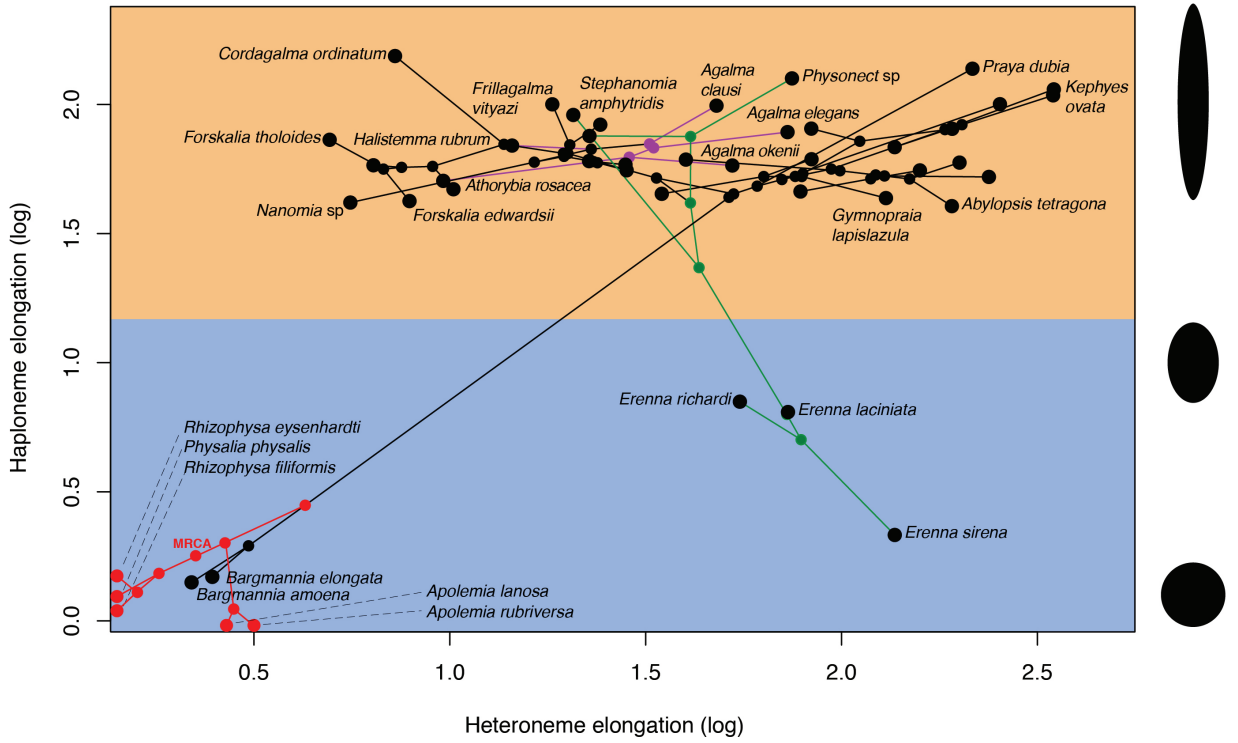


Figure 10: Phylomorphospace showing haploneme and heteroneme elongation (log scaled). Orange area delimits rod-shaped haplonemes, blue area covers oval and round shaped haplonemes. Smaller dots and lines represent phylogenetic relationships and ancestral states of internal nodes under BM. Species nodes in red were manually added to the plot. Cystonects have no tentacle heteronemes and are projected onto the haploneme axis. Apolemiids have no tentacle haplonemes and are projected onto the heteroneme axis. Colored branches and nodes correspond to BAMM regimes of accelerated haploneme shape (green) and heteroneme shape (violet) evolution.

515 identified two main independent regime shifts (Fig. 10): one in the branch leading to
516 Codonophora (anisorhizas diverging from cystonects' spherical isorhizas), and one in the
517 branch leading to Clade B physonects. Clade B includes *Erenna*, *Stephanomia*, *Marrus*, and
518 rhodaliids. Most of these taxa have rod-shaped anisorhizas, but *Erenna* has oval ones). No
519 clear regime shift patterns were identified in the evolution of desmoneme and rhopaloneme
520 shape.

521 *Functional morphology of tentillum and nematocyst discharge* – Tentillum and nematocyst
522 discharge high speed measurements are available in Appendix 4. While the sample sizes of
523 these measurements were insufficient to draw reliable statistical results at a phylogenetic level,
524 we did observe patterns that may be relevant to their functional morphology. For example,
525 cnidoband length is strongly correlated with discharge speed (p value = 0.0002). This is
526 probably the sole driver of the considerable difference between euphysonect and calycophoran
527 tentilla discharge speeds (average discharge speeds: 225.0mm/s and 41.8mm/s respectively;
528 t-test p value = 0.011), since the euphysonects have larger tentilla than the calycophorans
529 among the species recorded.

530 We also observed that calycophoran haploneme tubules fire faster than those of eu-
531 physonects (T-test p value = 0.001). Haploneme nematocysts discharge 2.8x faster than
532 heteroneme nematocysts (T-test p value = 0.0012). Finally, we observed that the stenoteles
533 of the Euphysonectae discharge a helical filament that “drills” itself through the medium it
534 penetrates as it everts.

535 Discussion

536 The core aims of this study are to examine the evolutionary history of siphonophore tentilla and
537 diet, characterize the evolutionary shifts in their trophic niches, and identify the morphological
538 characters that evolve with changes in prey type. We inquire whether the relationships between
539 form and function observed in extant taxa are due to correlated evolution or non-evolutionary
540 causes, whether the evolution of their trophic specializations supports or challenges traditional

541 ecological theory (such as the idea specialists evolve from generalists), and whether the diets
542 of siphonophores can be hypothesized by observing their tentacles. In addition, we produced
543 novel findings on tentillum morphology, siphonophore phylogeny, nematocyst character
544 evolution, and tentillum discharge dynamics.

545 *Evolution of tentillum morphology with diet* – Siphonophores are an abundant group of
546 zooplankton in oceanic ecosystems (Longhurst 1985; O’Brien 2007). While little is known
547 about siphonophore trophic ecology, what is known indicates that they occupy a central
548 position in midwater food webs (Choy et al. 2017), serving as trophic intermediaries between
549 smaller zooplankton and higher trophic level predators. Siphonophore species have been
550 observed to feed on a variety of prey with very different sizes, traits, and behaviors. Because
551 there is a total absence of siphonophores in the fossil record, how they became established
552 as the ubiquitous and diversified predators in today’s oceans remains an open question.
553 Predators that use morphologically similar tools for prey capture tend to capture similar prey,
554 thus their abundance and coexisting species diversity are inversely related due to competitive
555 exclusion by resource limitation (Schluter 2000). However, this is not consistent with what
556 we observe in siphonophores, which have been found to be both very abundant and locally
557 diverse (Longhurst 1985, @mapstone2014global). We hypothesize that siphonophores have
558 escaped this by specializing on different prey resources.

559 According to our reconstructions, the evolutionary history of siphonophore diets indicates
560 that being a specialist was an ancestral aspect of their trophic niche, while trophic generalism
561 is likely a derived condition. Several studies (reviewed in (Futuyma and Moreno 1988))
562 have suggested that resource specialization is an irreversible dead end due to the constraints
563 posed by phenotypic specialization. Our reconstructions show that this is not the case for
564 siphonophores, where the prey type on which they specialize has shifted at least 5 times, and
565 generalism has evolved independently at least twice. Among the evolutionary hypotheses
566 considered, we find support for both hypotheses 2 (specialist resource switching) and 3
567 (specialist to generalist), but no support for hypothesis 1 (generalist to specialist). The

568 evolutionary history of tentilla shows that siphonophores are an example of trophic niche
569 diversification via morphological innovation and evolution, which allowed transitions between
570 specialized trophic niches. This strategy is particularly important in a deep open ocean
571 ecosystem, which is a relatively homogeneous physical environment, where the primary niche
572 heterogeneity available is the potential interactions between organisms (Robison 2004).

573 One of the most common prey items found in siphonophore diets is copepods (Fig. 5).
574 Copepod-specialized diets have evolved convergently in *Cordagalma* and some calycophorans.
575 These evolutionary transitions happened together with transitions to smaller tentilla with
576 fewer cnidoband nematocysts. Tentilla are expensive single-use structures, therefore we would
577 expect that specialization in small prey would beget reductions in the size of the prey capture
578 apparatus to the minimum required for the ecological performance. *Cordagalma*'s tentilla
579 strongly resemble the larval tentilla (only found in the first-budded feeding body of the
580 colony) of their sister genus *Forskalia* spp. This indicates that the evolution of *Cordagalma*
581 tentilla could be a case of paedomorphosis associated with predatory specialization on smaller
582 prey.

583 (Purcell 1984) showed that haplonemes have a penetrating function as isorhizas in
584 cystonects and an adhesive function as anisorhizas in Tendiculophora. The two clades that
585 have been observed primarily feeding on fish (Cystonectae and Clade B, which includes
586 *Erenna*, *Stephanomia*, *Marrus*, and rhodaliids) present an accelerated rate of haploneme
587 shape evolution towards more compact haplonemes, significantly distinct from their closest
588 relatives. Isorhizas in cystonects are known to penetrate the skin of fish during prey capture,
589 and to deliver the toxins that aid in paralysis and digestion (Hessinger 1988). *Erenna*
590 anisorhizas are also able to penetrate human skin and deliver a painful sting (Pugh 2001)
591 (and pers. obs.), a common feature of piscivorous cnidarians like cystonects or cubozoans.

592 (Thomason 1988) hypothesized that smaller, more spherical nematocysts, with a lower
593 surface area to volume ratio, are more efficient in osmotic-driven discharge and thus have
594 more power for skin penetration. The elongated haplonemes of crustacean-eating Tendicu-

595 lophora have never been observed penetrating their crustacean prey ((Purcell 1984) and our
596 unpublished observations), and are hypothesized to entangle the prey through adhesion of
597 the abundant spines to the exoskeletal surfaces and appendages. Entangling requires less
598 acceleration and power during discharge than penetration, as it does not rely on point pressure.
599 In fish-eating cystonects and *Erenna* species, the haplonemes are much less elongated and
600 very effective at penetration, in congruence with the osmotic discharge hypothesis.

601 When we tested the diet-morphology correlation hypotheses supported in the literature
602 from a macroevolutionary perspective (Table 1), we found that most of them were consis-
603 tent with correlated evolution. The ecomorphological association between rhopalonemes,
604 desmonemes, and crustacean eaters was not congruent with a scenario of correlated evolution.
605 This is probably due to the broader set of taxa in our analyses, including multiple species
606 without desmonemes or rhopalonemes but which effectively capture crustaceans (such as
607 *Cordagalma ordinatum*, *Lychnagalma utricularia*, and *Bargmannia amoena*).

608 While our results unambiguously show that tentillum morphology evolved with diet, the
609 conclusions we can draw from these analyses are limited by the sparse dietary data available.
610 Moreover, our analyses are not sufficient to adequately test hypotheses of adaptation, since
611 that would require evidence of changes within a population exposed to different selective
612 pressures. When interpreting these results, it is important to remember that diet is a product
613 of environmental prey availability and predator selectivity. Selectivity differences across
614 siphonophore species could be driven by other phenotypes not accounted for this study. For
615 example, tentacle-deploying behavior, positioning in the water column, sensitivity thresholds
616 for nematocyst discharge, or chemical cues to ingest a captured animal. Further observations
617 on these behaviors in the field are necessary to assess their relative importance in determining
618 dietary composition. In addition to behavior, there is much biochemistry in the prey capture
619 and digestion processes that remains unexplored. Part of the success in siphonophore prey
620 capture is likely determined by the effectivity of the toxins delivered by the nematocysts
621 on different taxa. Comparative toxin assays and venom protein evolution studies would

shed light on this question. Moreover, siphonophore trophic specialization may have brought changes in the digestive biochemistry of gastrozooids and palpons. A comparison of the gene expression levels for different enzymes in the gastrozooids of different species, together with digestive enzyme sequence evolution studies, and a toxicological assay of the different venoms in siphonophore nematocysts on different prey taxa, would provide a great complement to our results.

Generating hypotheses on siphonophore feeding ecology – One motivation for our research was to understand the links between predator capture tools and their diets so we can generate hypotheses about the diets of siphonophores based on morphological characteristics. Indeed, our discriminant analyses were able to distinguish between different siphonophore diets based on morphological characters alone. The models produced by these analyses generated testable predictions about the diets of many species for which we only have morphological data of their tentacles. While the limited dataset used here is informative for generating tentative hypotheses, the empirical dietary data are still scarce and insufficient to cast robust predictions. This reveals the need to extensively characterize siphonophore diets and feeding habits. In future work, we can test these ecological hypotheses and validate these models by directly characterizing the diets of some of those siphonophore species. Predicting diet using morphology is a powerful tool to reconstruct food web topologies from community composition alone. In many of the ecological models found in the literature, interactions among the oceanic zooplankton have been treated as a black box (Mitra 2009). The ability to predict such interactions, including those of siphonophores and their prey, will enhance the taxonomic resolution of nutrient-flow models constructed from plankton community composition data.

Phenotypic integration of siphonophore tentilla – Many tentillum characters, such as nematocysts, arose from the subfunctionalization of serial homologs (David et al. 2008). Serial homologs have shared genetic elements underlying their development, and are expected to have phylogenetic correlations (Wagner and Schwenk 2000). In addition, these sub-structures

649 must fit and work together in synchrony to ensnare prey successfully (functional integration).
650 Character complexes that satisfy these conditions tend to be phenotypically integrated.
651 Phenotypic integration is the set of functional and genetic correlations among the traits of an
652 organism (Pigliucci 2003). These correlations have been hypothesized to direct and constrain
653 adaptive evolution (Wagner and Schwenk 2000). The siphonophore tentillum morphospace
654 has a fairly low extant dimensionality due to an evolutionary history with many synchronous,
655 correlated changes. This is consistent with strong phenotypic integration where genetic and
656 developmental correlations are maintained by natural selection to preserve function.

657 Structural correlations within the tentillum are expected from shared regulatory networks
658 within a common developmental bud (budding tentilla in the tentacle). Similarly, correlations
659 between nematocyst subtypes are also expected given their common evolutionary and develop-
660 mental origin. None of these explanations for correlated evolution are surprising, nor require
661 natural selection. However, we also found correlations between nematocyst and tentillum
662 characters. Siphonophore tentacle nematocysts (in their cnidocytes) are not produced nor
663 matured in the developing tentillum. These cnidocytes are produced by dividing cnidoblasts
664 in the basigaster (basal swelling of the gastrozooid). Once the cnidocytes have assembled the
665 nematocyst, they migrate outward along the tentacle (Carré 1972) and position themselves
666 in the tentillum according to their type and size (Skaer 1988). Thus, the developmental pro-
667 grams that produce the observed nematocyst morphologies are spatially separated from those
668 producing the tentillum morphologies. Therefore, we hypothesize the genetic correlations and
669 phenotypic integration between tentillum and nematocyst characters are maintained through
670 natural selection on separate regulatory networks, out of the necessity to work together and
671 meet the spatial, mechanical, and functional constraints of their prey capture behavior.

672 Our evolutionary rate covariance results indicate that tentilla are not only phenotypically
673 integrated, but also show patterns of evolutionary modularity, where different sets of characters
674 appear to evolve in stronger correlations among each other than with other characters. This
675 may be indicative of the underlying genetic and developmental dependencies among closely

676 homologous nematocyst types (such as desmonemes and rhopalonemes) and structures. In
677 addition, these evolutionary modules point to hypothetical functional modules. For example,
678 the coiling degree of the cnidoband and the extent of the involucrum have correlated rates of
679 evolution, while high speed videos show that the involucrum helps direct the whiplash of the
680 uncoiling cnidoband forward (towards the prey).

681 While selection acting on character states is a widely studied phenomenon, recent studies
682 have shown that selection can also act upon the patterns of character correlations and
683 phenotypic dependencies (Young and HallgrÍmsson 2005; Goswami 2006; Revell and Collar
684 2009; Monteiro and Nogueira 2010; Hallgrí'msson et al. 2012; Claverie and Patek 2013;
685 Caetano and Harmon 2018). This evolution of character relationships can allow lineages
686 to explore new regions of the morphospace and facilitate the appearance of ecological
687 novelties. Our results show that the patterns of phenotypic integration in siphonophore
688 tentilla vary among clades, and appear to display different relationships across shifting feeding
689 specializations. Similarly to what has been found in the feeding morphologies of fish (Collar
690 et al. 2005; Revell and Collar 2009), siphonophore tentilla may have accommodated new diets
691 by altering the correlations between characters. For example, changes in the size and shape
692 relationships between nematocyst types gave rise to the nematocyst complements specialized
693 in ensnaring small crustaceans or fish. Finally, the evolvability of phenotypic dependencies
694 likely had a large role in the evolution of the diverse tentilla morphologies we observe today
695 across siphonophores.

696 *Evolutionary history of tentillum morphology* – This study produced the most speciose
697 siphonophore molecular phylogeny to date, while incorporating the most recent findings
698 in siphonophore deep node relationships. This phylogeny revealed for the first time that
699 the genus *Erenna* is the sister to *Stephanomia amphytridis*. *Erenna* and *Stephanomia* bear
700 the largest tentilla among all siphonophores, thus their monophyly indicates that there was
701 a single evolutionary transition to giant tentilla. Siphonophore tentilla range in size from
702 ~30 µm in some *Cordagalma* specimens to 2-4 cm in *Erenna* species, and up to 8 cm in

Stephanomia amphytridis (Pugh and Baxter 2014). Most siphonophore tentilla measure between 175 and 1007 µm (1st and 3rd quartiles), with a median of 373 µm. The extreme gain of tentillum size in this newly found clade may have important implications for access to large prey size classes.

Tentillum size, as well as the majority of the characters studied, supported BM evolutionary models. There are two alternative hypotheses about the generative process of BM. One hypothesis would suggest that these characters are not under selection, and therefore diverging neutrally (Lande 1976). The second hypothesis suggests that they are under selection, but the adaptive landscape was rapidly shifting (Hansen and Martins 1996), without leaving clear patterns across the phylogeny. Some of the BM supported characters are likely to have evolved under the second hypothesis, since when a diet-driven regime tree was provided, these characters preferentially supported an OU model (Appendix 14).

Siphonophore tentilla are defined as lateral, monostichous evaginations of the tentacle gastrovascular lumen with epidermal nematocysts (Totton and Bargmann 1965). The buttons on *Physalia* tentacles were not traditionally regarded as tentilla, but (Bardi and Marques 2007) and our observations (Munro et al. 2018), confirm that the buttons contain evaginations of the gastrovascular lumen, thus satisfying all the criteria for the definition. In this light, and given that most Cystonectae bear conspicuous tentilla, we conclude (in agreement with (Munro et al. 2018)) that tentilla are likely ancestral to all siphonophores, and secondarily lost in *Apolemia* and *Bathyphysa conifera*.

The clade Tendiculophora contains far more species than its relatives Cystonectae, Apolemiidae, and Pyrostephidae. An increase in clade richness and ecological diversification can be triggered by a ‘key innovation’ (Simpson 1955). The evolutionary innovation of the Tendiculophora tentilla with shooting cnidobands and modular regions may have facilitated further dietary diversification. In addition, our work identifies an interesting example of convergent evolution. The region of the tentillum morphospace (Fig. 9) occupied by calycophorans was independently (and more recently) occupied by the physonect *Frillagalma vityazi*. Like caly-

730 cophorans, *Frillagalma* tentilla have small C-shaped cnidobands with a few rows of anisorhizas.
731 Unlike calycophorans, they lack paired elongate microbasic mastigophores. Instead, they
732 bear three elongated stenoteles, and their cnidobands are followed by a branched vesicle,
733 unique to this genus. Their tentillum morphology is very different from that of other related
734 physonects, which tend to have long, coiled, cnidobands with many paired oval stenoteles.
735 Most studies on calycophoran diets have reported their prey to be primarily composed of
736 small crustaceans, such as copepods or ostracods (Purcell 1981, 1984). The diet of *Frillagalma*
737 *vityazi* is unknown, but this morphological convergence suggests that they evolved to capture
738 similar kinds of prey. Our DAPCs predict that *Frillagalma* has a generalist niche with both
739 soft and hard bodied prey, including copepods.

740 *Evolution of nematocyst shape* – The phylogenetic placement of siphonophores among the
741 Hydrozoa remains an unresolved question (Munro et al. 2018). The most recent work on
742 this front sets them as sister group to all other Hydroidolina (Kayal et al. 2015). Therefore,
743 there is a great uncertainty around the ancestral plesiomorphies of the common ancestor
744 of all siphonophores. This is especially true for those characters that present extreme
745 differences between Cystonectae and Codonophora (the earliest split in the siphonophore
746 phylogeny). One such character is the shape of haploneme nematocysts. A remarkable
747 feature of siphonophore haplonemes is that they are outliers to all other Medusozoa in
748 their surface area to volume relationships, deviating significantly from sphericity (Thomason
749 1988). This suggests a different mechanism for their discharge that could be more reliant on
750 capsule tension than on osmotic potentials (Carré and Carré 1980), and strong selection for
751 efficient nematocyst packing in the cnidoband (Thomason 1988; Skaer 1988). Our results
752 show that Codonophora underwent a shift towards elongation and Cystonectae towards
753 sphericity, assuming the common ancestor had an intermediate state. Since we know that
754 the haplonemes of other hydrozoan outgroups are generally spheroid, it is more parsimonious
755 to assume that cystonects retain this ancestral state. Later, we observe a return to more
756 rounded (ancestral) haplonemes in *Erenna*, concurrent with a secondary gain of a piscivorous

757 trophic niche, like that exhibited by cystonects.

758 In parallel with haploneme shape, heteroneme shape evolution also presents a single,
759 large, early transition towards elongation. While cystonects do not bear heteronemes in their
760 tentacles, *Physalia physalis* bears stenoteles in other zooids (Totton and Bargmann 1965),
761 hypothetically used for defense rather than for prey capture. These stenotele heteronemes are
762 rounded like those found in pyrostephids and apolemiids, which is consistent with the story
763 of a single transition leading to the elongated heteronemes in the stem of Tendiculophora.

764 The implications of these results to the evolution of nematocyst function are that an
765 innovation in the discharge mechanism of haplonemes may have occurred during the main shift
766 to elongation. Elongate nematocysts can be tightly packed into cnidobands. We hypothesize
767 this may be a Tendiculophora lineage-specific adaptation to packing more nematocysts into
768 a limited tentillum space, as suggested by (Skaer 1988). Tendiculophora, comprised of
769 the clades Euphysonectae and Calycophorae, includes the majority of siphonophore species.
770 Among these, are the most abundant siphonophore species, and a greater morphological and
771 ecological diversity is found. We hypothesize that this packing-efficient haploeme morphology
772 may have been a key innovation leading to the diversification of this clade. However, other
773 characters that shifted concurrently in the stem of this clade may have been responsible for
774 their extant diversity.

775 Some siphonophore clades have more nematocyst types than others in the tentacles
776 (Tendiculophora has 4 types, Cystonectae and Apolemiidae have 1), or different subtypes
777 (e.g. stenoteles, mastigophores, birhopaloids). In addition to the tentacles, siphonophores
778 may bear nematocysts in other parts of the colony (gastrozooids, papons, palpacles, bracts,
779 nectophores, and gonozoooids) (Totton and Bargmann 1965). In this paper we only look at
780 the presence of nematocyst types in the tentacles, therefore the gains and losses reported
781 are not necessarily morphological innovations, but developmental allocations. Nonetheless,
782 siphonophores have evolved unique nematocyst types and subtypes, not present in any other
783 cnidarian, such as the two types of rhopalonemes (acrophores and anacrophores), and the

784 haploneme homotrichous anisorrhizas (Werner 1965). Both these nematocyst types evolved in
785 the stem to Tendiculophora, and are likely morphological innovations, since they have not
786 yet been found in any other tissue of any other organism. The gain of extreme elongation in
787 the haplonemes of Tendiculophora can be interpreted as part of the character shift to a novel
788 anisorrhiza subtype.

789 *Diversity of discharge dynamics* – A fundamental corollary in functional morphology is
790 that structural morphology determines functional performance (Wainwright and Reilly 1994).
791 We expected the discharge dynamics exhibited by siphonophore tentilla should vary with their
792 morphological diversity. Our results are consistent with this expectation, and we observe,
793 for example, that cnidoband size largely correlates with cnidoband discharge speed. This
794 suggests that prey escape response speed may determine the minimum cnidoband length for
795 successful capture.

796 *Insights from tentillum morphology* – The measurements taken illustrate that the mor-
797 phological diversity of siphonophore tentilla and nematocysts is remarkable, both in their
798 range of shapes and sizes, as in the dimensions and subtypes of the nematocysts they bear.
799 Siphonophores bear the largest nematocysts among Hydrozoans. The largest nematocysts
800 in our dataset (*Bargmannia lata* by volume and *Resomia dunnii* by length), are the largest
801 of all nematocysts reported for cnidarians, and therefore possibly the largest intracellular
802 organelles among all living things.

803 In addition to the insights produced in this study, the newly collected morphological
804 data provide a unique resource for future studies, and a reference dataset for siphonophore
805 identification. Many conspicuous categorical characters in siphonophore tentilla are singularly
806 diagnostic, such as: the fluorescent lures of *Resomia ornicephala*, the bioluminescent lures
807 of *Erenna* species, the unique branched vesicle of *Frillagalma vityazi*, the buoyant medusa-
808 resembling vesicle of *Lychnagalma* with 8 pseudo-tentacles, the zig-zag morphology of *Resomia*
809 species, the inverted orientation of *Physophora* cnidobands, the button-like tentilla of *Physalia*,
810 or the acorn-shaped minute tentilla of *Cordagalma* species (Fig. 7). Some categorical

811 characters are synapomorphic diagnostic characters for large clades, such as the proximal
812 tentillum heteronemes of Eucladophora, the elastic strand, rhopalonemes, and desmonemes of
813 Tendiculophora, the larval tentilla of Euphysonectae, the two-sized isorhizas of Cystonectae,
814 the saccus canal of Pyrostephidae, or the seven rows of anisorhizas in Calycophorae. These
815 characters should be used together with the classical nectophore and bract characters to
816 identify species or at least impute phylogenetic affiliation from incomplete material.

817 **Conclusions**

818 Siphonophores have diverse predatory niches in the open ocean, ranging from mid-trophic
819 small crustacean eaters to piscivorous super-carnivores. With the evolution of diversified
820 prey type specializations comes the evolution of morphologies adapted to the challenges
821 posed by different prey. The results presented here indicate that the associations found
822 between siphonophore tentilla and their prey are a product of correlated evolution in highly
823 integrated traits. While much of the literature focuses on how predatory generalists evolve
824 into predatory specialists, in siphonophores we find predatory specialists can evolve into
825 generalists, and that specialists on one prey type have directly evolved into specialists on
826 other prey types. Our extended morphological characterization shows that the relationships
827 between form and ecology hold across a large set of taxa and characters, and can be used to
828 generate hypotheses on the feeding habits of uncharacterized species. We conclude that the
829 siphonophores were able to become abundant oceanic predators by occupying a variety of
830 trophic niches facilitated by the evolution and diversification of extraordinary prey capture
831 tools on their tentacles.

832 **Supplementary Materials**

833 Data available from the Dryad Digital Repository: <http://dx.doi.org/10.5061/dryad.NNNN>
834 Online Appendices are available in https://github.com/dunnlab/tentilla_morph/
835 Supplementary_materials/Online_Appendices

⁸³⁶ **Funding**

⁸³⁷ This work was supported by the Society of Systematic Biologists (Graduate Student Award
⁸³⁸ to A.D.S.); the Yale Institute of Biospheric Studies (Doctoral Pilot Grant to A.D.S.); and
⁸³⁹ the National Science Foundation (Waterman Award to C.W.D., and NSF-OCE 1829835 to
⁸⁴⁰ C.W.D., S.H.D.H., and C. Anela Choy). A.D.S. was supported by a Fulbright Spain Graduate
⁸⁴¹ Studies Scholarship.

⁸⁴² **Acknowledgements**

⁸⁴³ We wish to thank the crew and scientists of the R/V Western Flyer, who participated in
⁸⁴⁴ the collection of many of the specimens used in this study. We also want to thank Lynne
⁸⁴⁵ Christianson and Shannon Johnson from the Monterey Bay Aquarium Research Institute
⁸⁴⁶ for their assistance in the field as well as for sequencing some of the species included in this
⁸⁴⁷ phylogeny. In addition, we wish to thank Lourdes Rojas, Daniel Drew, and Eric Lazo-Wasem
⁸⁴⁸ for their assistance in imaging the fixed specimens and managing the collections. We thank
⁸⁴⁹ Dennis Pilarczyk for organizing the prey selectivity data, and Joaquin Nunez for reviewing
⁸⁵⁰ this manuscript. Furthermore, we thank Elizabeth D. Hetherington and C. Anela Choy
⁸⁵¹ for collating the data on siphonophore feeding and for reviewing the manuscript. Finally,
⁸⁵² we thank Philip Pugh, who confirmed many of our specimen identifications and taught us
⁸⁵³ valuable knowledge about siphonophores.

⁸⁵⁴ **References**

- ⁸⁵⁵ Andersen O.G.N. 1981. Redescription of marrus orthocanna (kramp, 1942)(Cnidaria,
⁸⁵⁶ siphonophora). Zoological Museum, University of Copenhagen.
- ⁸⁵⁷ Bardi J., Marques A.C. 2007. Taxonomic redescription of the portuguese man-of-war,
⁸⁵⁸ physalia physalis (cnidaria, hydrozoa, siphonophorae, cystonectae) from brazil. Iheringia.
⁸⁵⁹ Série Zoologia. 97:425–433.

- 860 Beaulieu J., O'Meara B. 2012. OUwie: Analysis of evolutionary rates in an ou framework.
- 861 R package version 1.17..
- 862 Biggs D.C. 1977. Field studies of fishing, feeding, and digestion in siphonophores. *Marine*
- 863 & Freshwater Behaviour & Phy. 4:261–274.
- 864 Blomberg S.P., Garland T., Ives A.R. 2003. Testing for phylogenetic signal in comparative
- 865 data: Behavioral traits are more labile. *Evolution*. 57:717–745.
- 866 Blyth C.R. 1972. On simpson's paradox and the sure-thing principle. *Journal of the*
- 867 American Statistical Association. 67:364–366.
- 868 Butler M.A., King A.A. 2004. Phylogenetic comparative analysis: A modeling approach
- 869 for adaptive evolution. *The American Naturalist*. 164:683–695.
- 870 Caetano D.S., Harmon L.J. 2018. Estimating correlated rates of trait evolution with
- 871 uncertainty. *Systematic biology*. 68:412–429.
- 872 Carré D. 1972. Study on development of cnidocysts in gastrozooids of muggiaeae kochi
- 873 (will, 1844) (siphonophora, calycophora). *Comptes Rendus Hebdomadaires des Seances de*
- 874 l'Academie des Sciences Serie D. 275:1263.
- 875 Carré D., Carré C. 1980. On triggering and control of cnidocyst discharge. *Marine &*
- 876 Freshwater Behaviour & Phy. 7:109–117.
- 877 Choy C.A., Haddock S.H., Robison B.H. 2017. Deep pelagic food web structure as revealed
- 878 by in situ feeding observations. *Proceedings of the Royal Society B: Biological Sciences*.
- 879 284:20172116.
- 880 Claverie T., Patek S. 2013. Modularity and rates of evolutionary change in a power-
- 881 amplified prey capture system. *Evolution*. 67:3191–3207.
- 882 Collar D.C., Near T.J., Wainwright P.C. 2005. Comparative analysis of morphological
- 883 diversity: Does disparity accumulate at the same rate in two lineages of centrarchid fishes?
- 884 *Evolution*. 59:1783–1794.
- 885 Collins T.J. 2007. ImageJ for microscopy. *Biotechniques*. 43:S25–S30.
- 886 Costello J.H., Colin S.P., Gemmell B.J., Dabiri J.O., Sutherland K.R. 2015. Multi-jet

- propulsion organized by clonal development in a colonial siphonophore. *Nature communications.* 6:8158.
- Cressler C.E., Butler M.A., King A.A. 2015. Detecting adaptive evolution in phylogenetic comparative analysis using the ornstein–uhlenbeck model. *Systematic biology.* 64:953–968.
- David C.N., Özbek S., Adamczyk P., Meier S., Pauly B., Chapman J., Hwang J.S., Gojobori T., Holstein T.W. 2008. Evolution of complex structures: Minicollagens shape the cnidarian nematocyst. *Trends in genetics.* 24:431–438.
- Dunn C.W., Pugh P.R., Haddock S.H. 2005. Molecular phylogenetics of the siphonophora (cnidaria), with implications for the evolution of functional specialization. *Systematic biology.* 54:916–935.
- Felsenstein J. 1985. Phylogenies and the comparative method. *The American Naturalist.* 125:1–15.
- Futuyma D.J., Moreno G. 1988. The evolution of ecological specialization. *Annual review of Ecology and Systematics.* 19:207–233.
- Goswami A. 2006. Morphological integration in the carnivoran skull. *Evolution.* 60:169–183.
- Grafen A. 1989. The phylogenetic regression. *Philosophical Transactions of the Royal Society of London. B, Biological Sciences.* 326:119–157.
- Haddock S.H., Dunn C.W. 2015. Fluorescent proteins function as a prey attractant: Experimental evidence from the hydromedusa olindias formosus and other marine organisms. *Biology open.* 4:1094–1104.
- Haddock S.H., Dunn C.W., Pugh P.R., Schnitzler C.E. 2005. Bioluminescent and red-fluorescent lures in a deep-sea siphonophore. *Science.* 309:263–263.
- Haddock S.H., Heine J.N. 2005. Scientific blue-water diving. California Sea Grant College Program.
- Hallgrímsisson B., Jamniczky H.A., Young N.M., Rolian C., SCHMIDT-OTT U., Marcucio R.S. 2012. The generation of variation and the developmental basis for evolutionary novelty.

- 914 Journal of Experimental Zoology Part B: Molecular and Developmental Evolution. 318:501–
915 517.
- 916 Hansen T.F., Martins E.P. 1996. Translating between microevolutionary process and
917 macroevolutionary patterns: The correlation structure of interspecific data. Evolution.
918 50:1404–1417.
- 919 Hardin G. 1960. The competitive exclusion principle. science. 131:1292–1297.
- 920 Harmon L.J., Losos J.B., Jonathan Davies T., Gillespie R.G., Gittleman J.L., Bryan
921 Jennings W., Kozak K.H., McPeek M.A., Moreno-Roark F., Near T.J., others. 2010. Early
922 bursts of body size and shape evolution are rare in comparative data. Evolution: International
923 Journal of Organic Evolution. 64:2385–2396.
- 924 Harmon L.J., Weir J.T., Brock C.D., Glor R.E., Challenger W. 2007. GEIGER: Investi-
925 gating evolutionary radiations. Bioinformatics. 24:129–131.
- 926 Hessinger D.A. 1988. Nematocyst venoms and toxins. The biology of nematocysts.
927 Elsevier. p. 333–368.
- 928 Hissmann K. 2005. In situ observations on benthic siphonophores (physonectae: Rhodali-
929 idae) and descriptions of three new species from indonesia and south africa. Systematics and
930 Biodiversity. 2:223–249.
- 931 Hoberg E.P., Brooks D.R. 2008. A macroevolutionary mosaic: Episodic host-switching,
932 geographical colonization and diversification in complex host–parasite systems. Journal of
933 Biogeography. 35:1533–1550.
- 934 Höhna S., Landis M.J., Heath T.A., Boussau B., Lartillot N., Moore B.R., Huelsenbeck
935 J.P., Ronquist F. 2016. RevBayes: Bayesian phylogenetic inference using graphical models
936 and an interactive model-specification language. Systematic Biology. 65:726–736.
- 937 Hutchinson G.E. 1961. The paradox of the plankton. The American Naturalist. 95:137–
938 145.
- 939 Jacobs J. 1974. Quantitative measurement of food selection. Oecologia. 14:413–417.
- 940 Johnson K.P., Malenke J.R., Clayton D.H. 2009. Competition promotes the evolution of

- 941 host generalists in obligate parasites. *Proceedings of the Royal Society B: Biological Sciences*.
942 276:3921–3926.
- 943 Jombart T., Devillard S., Balloux F. 2010. Discriminant analysis of principal components:
944 A new method for the analysis of genetically structured populations. *BMC genetics*. 11:94.
- 945 Kalyaanamoorthy S., Minh B.Q., Wong T.K., Haeseler A. von, Jermiin L.S. 2017. Mod-
946 elFinder: Fast model selection for accurate phylogenetic estimates. *Nature methods*. 14:587.
- 947 Katoh K., Misawa K., Kuma K.-i., Miyata T. 2002. MAFFT: A novel method for
948 rapid multiple sequence alignment based on fast fourier transform. *Nucleic acids research*.
949 30:3059–3066.
- 950 Kayal E., Bentlage B., Cartwright P., Yanagihara A.A., Lindsay D.J., Hopcroft R.R.,
951 Collins A.G. 2015. Phylogenetic analysis of higher-level relationships within hydrodolina
952 (cnidaria: Hydrozoa) using mitochondrial genome data and insight into their mitochondrial
953 transcription. *PeerJ*. 3:e1403.
- 954 Lande R. 1976. Natural selection and random genetic drift in phenotypic evolution.
955 *Evolution*. 30:314–334.
- 956 Longhurst A.R. 1985. The structure and evolution of plankton communities. *Progress in*
957 *Oceanography*. 15:1–35.
- 958 Mackie G.O., Pugh P.R., Purcell J.E. 1987. Siphonophore Biology. *Advances in Marine*
959 *Biology*. 24:97–262.
- 960 Mapstone G.M. 2014. Global diversity and review of siphonophorae (cnidaria: Hydrozoa).
961 *PLoS One*. 9:e87737.
- 962 Martins E.P. 1996. Phylogenies, spatial autoregression, and the comparative method: A
963 computer simulation test. *Evolution*. 50:1750–1765.
- 964 Mitra A. 2009. Are closure terms appropriate or necessary descriptors of zooplankton loss
965 in nutrient–phytoplankton–zooplankton type models? *Ecological Modelling*. 220:611–620.
- 966 Monteiro L.R., Nogueira M.R. 2010. Adaptive radiations, ecological specialization, and
967 the evolutionary integration of complex morphological structures. *Evolution: International*

- 968 Journal of Organic Evolution. 64:724–744.
- 969 Munro C., Siebert S., Zapata F., Howison M., Serrano A.D., Church S.H., Goetz F.E.,
- 970 Pugh P.R., Haddock S.H., Dunn C.W. 2018. Improved phylogenetic resolution within
- 971 siphonophora (cnidaria) with implications for trait evolution. Molecular Phylogenetics and
- 972 Evolution.
- 973 Nguyen L.-T., Schmidt H.A., Haeseler A. von, Minh B.Q. 2014. IQ-tree: A fast and
- 974 effective stochastic algorithm for estimating maximum-likelihood phylogenies. Molecular
- 975 biology and evolution. 32:268–274.
- 976 O’Brien T.D. 2007. COPEPOD, a global plankton database: A review of the 2007
- 977 database contents and new quality control methodology..
- 978 Pagel M. 1994. Detecting correlated evolution on phylogenies: A general method for the
- 979 comparative analysis of discrete characters. Proceedings of the Royal Society of London.
- 980 Series B: Biological Sciences. 255:37–45.
- 981 Paradis E., Blomberg S., Bolker B., Brown J., Claude J., Cuong H.S., Desper R. 2019.
- 982 Package “ape”. Analyses of phylogenetics and evolution, version.:2–4.
- 983 Pennell M.W., FitzJohn R.G., Cornwell W.K., Harmon L.J. 2015. Model adequacy and
- 984 the macroevolution of angiosperm functional traits. The American Naturalist. 186:E33–E50.
- 985 Pigliucci M. 2003. Phenotypic integration: Studying the ecology and evolution of complex
- 986 phenotypes. Ecology Letters. 6:265–272.
- 987 Pugh P. 2001. A review of the genus erenna bedot, 1904 (siphonophora, physonectae).
- 988 BULLETIN-NATURAL HISTORY MUSEUM ZOOLOGY SERIES. 67:169–182.
- 989 Pugh P., Baxter E. 2014. A review of the physonect siphonophore genera halistemma
- 990 (family agalmatidae) and stephanomia (family stephanomiidae). Zootaxa. 3897:1–111.
- 991 Pugh P., Youngbluth M. 1988. Two new species of prayine siphonophore (calycophorae,
- 992 prayidae) collected by the submersibles johnson-sea-link i and ii. Journal of Plankton Research.
- 993 10:637–657.
- 994 Purcell J. 1981. Dietary composition and diel feeding patterns of epipelagic siphonophores.

- 995 Marine Biology. 65:83–90.
- 996 Purcell J.E. 1980. Influence of siphonophore behavior upon their natural diets: Evidence
997 for aggressive mimicry. Science. 209:1045–1047.
- 998 Purcell J.E. 1984. The functions of nematocysts in prey capture by epipelagic
999 siphonophores (coelenterata, hydrozoa). The Biological Bulletin. 166:310–327.
- 1000 Purcell J., Mills C. 1988. The correlation of nematocyst types to diets in pelagic hydrozoa.
1001 In “the biology of nematocysts”.(Eds da hessinger and hm lenhoff.) pp. 463–485..
- 1002 Rabosky D.L., Grundler M., Anderson C., Title P., Shi J.J., Brown J.W., Huang H.,
1003 Larson J.G. 2014. BAMM tools: An r package for the analysis of evolutionary dynamics on
1004 phylogenetic trees. Methods in Ecology and Evolution. 5:701–707.
- 1005 Revell L.J. 2012. Phytools: An r package for phylogenetic comparative biology (and other
1006 things). Methods in Ecology and Evolution. 3:217–223.
- 1007 Revell L.J., Chamberlain S.A. 2014. Rphylip: An r interface for phylip. Methods in
1008 Ecology and Evolution. 5:976–981.
- 1009 Revell L.J., Collar D.C. 2009. Phylogenetic analysis of the evolutionary correlation using
1010 likelihood. Evolution: International Journal of Organic Evolution. 63:1090–1100.
- 1011 Robison B.H. 2004. Deep pelagic biology. Journal of experimental marine biology and
1012 ecology. 300:253–272.
- 1013 Schindelin J., Arganda-Carreras I., Frise E., Kaynig V., Longair M., Pietzsch T., Preibisch
1014 S., Rueden C., Saalfeld S., Schmid B., others. 2012. Fiji: An open-source platform for
1015 biological-image analysis. Nature methods. 9:676.
- 1016 Schluter D. 2000. Ecological character displacement in adaptive radiation. the american
1017 naturalist. 156:S4–S16.
- 1018 Schmitz O. 2017. Predator and prey functional traits: Understanding the adaptive
1019 machinery driving predator–prey interactions. F1000Research. 6.
- 1020 Shapiro S.S., Wilk M.B. 1965. An analysis of variance test for normality (complete
1021 samples). Biometrika. 52:591–611.

- 1022 Siebert S., Pugh P.R., Haddock S.H., Dunn C.W. 2013. Re-evaluation of characters in
1023 apolemiidae (siphonophora), with description of two new species from monterey bay, california.
1024 Zootaxa. 3702:201–232.
- 1025 Simpson G.G. 1944. Tempo and mode in evolution. Columbia University Press.
- 1026 Simpson G.G. 1955. Major features of evolution. Columbia University Press: New York.
- 1027 Skaer R. 1988. The formation of cnidocyte patterns in siphonophores. Academic Press
1028 New York.
- 1029 Skaer R. 1991. Remodelling during the development of nematocysts in a siphonophore.
1030 Hydrobiologia. 216:685–689.
- 1031 Stireman-III J.O. 2005. The evolution of generalization? Parasitoid flies and the perils of
1032 inferring host range evolution from phylogenies. Journal of evolutionary biology. 18:325–336.
- 1033 Sugiura N. 1978. Further analysts of the data by akaike's information criterion and the
1034 finite corrections: Further analysts of the data by akaike's. Communications in Statistics-
1035 Theory and Methods. 7:13–26.
- 1036 Team R.C. 2017. R: A language and environment for statistical computing. Vienna,
1037 austria: R foundation for statistical computing; 2017..
- 1038 Thomason J. 1988. The allometry of nematocysts. The biology of nematocysts. Elsevier.
1039 p. 575–588.
- 1040 Totton A.K., Bargmann H.E. 1965. A synopsis of the siphonophora. British Museum
1041 (Natural History).
- 1042 Uhlenbeck G.E., Ornstein L.S. 1930. On the theory of the brownian motion. Physical
1043 review. 36:823.
- 1044 Uyeda J.C., Zenil-Ferguson R., Pennell M.W. 2018. Rethinking phylogenetic comparative
1045 methods. Systematic Biology. 67:1091–1109.
- 1046 Wagner G.P., Schwenk K. 2000. Evolutionarily stable configurations: Functional in-
1047 tegration and the evolution of phenotypic stability. Evolutionary biology. Springer. p.
1048 155–217.

- 1049 Wainwright P.C., Reilly S.M. 1994. Ecological morphology: Integrative organismal biology.
- 1050 University of Chicago Press.
- 1051 Werner B. 1965. Die nesselkapseln der cnidaria, mit besonderer berücksichtigung der
- 1052 hydroida. Helgoländer wissenschaftliche Meeresuntersuchungen. 12:1.
- 1053 Young N.M., Hallgrímsson B. 2005. Serial homology and the evolution of mammalian
- 1054 limb covariation structure. Evolution. 59:2691–2704.